CATÓLICA

UNIVERSIDADE CATÓLICA PORTUGUESA | PORTO

Escola Superior de Biotecnologia

Calcium Phosphate Cements reinforced with Polyvinyl Alcohol fibers for bone load-bearing applications

by

Tomás Sobral Marques

June 2016

CATÓLICA
UNIVERSIDADE CATÓLICA PORTUGUESA | PORTO
Escola Superior de Biotecnologia

Calcium Phosphate Cements reinforced with Polyvinyl Alcohol fibers for bone load-bearing applications

Chemical, mechanical and biological characterization

Thesis presented to *Escola Superior de Biotecnologia* of the *Universidade Católica Portuguesa* to fulfill the requirements of Master of Science degree in Biomedical Engineering

by
Tomás Sobral Marques

Place: Radboud University Medical Center

Supervision: Dr. Sander Leeuwenburgh, associate professor
Sónia Schickert, PhD student

June 2016

To my parents and my brother Tiago, who are having a determinant role in my personal values.

resumo

O desenvolvimento de biocerâmicos para a regeneração do tecido ósseo tem sido amplamente explorado, dada a sua elevada frequência de transplantação resultante de problemas associados a defeitos congénitos, doenças ósseas ou situações traumáticas. Neste âmbito, desde 1980 que os cimentos de fosfato de cálcio tem desempenhado um papel importante como substituintes do osso ou como material de suporte para a regeneração óssea, apresentando boas propriedades ao nível da biocompatibilidade e bioatividade. Contudo, as propriedades mecânicas desta categoria de biocerâmicos apresentam limitações no que respeita à fragilidade e à reduzida resistência à flexão. Como tal, as zonas de possível aplicação destes cimentos estão limitadas a regiões de suporte de cargas mecânicas reduzidas.

O reforço de cimentos com fibras poliméricas, é uma solução desde há muito amplamente explorada pela engenharia civil, no sentido de melhorar as propriedades mecânicas dos cimentos, aumentando a sua ductilidade. Do mesmo principio de engenharia, para reforçar compósitos com fins médicos, polímeros de origem natural e sintética tem sido estudados. Resultados promissores *in vitro* e *in vivo* já foram alcançados, contudo não satisfatórios para aplicação em áreas cujas cargas a suportar são elevadas.

O polivinil álcool é um polímero utilizado no reforço de compósitos, dado as suas reconhecidas propriedades mecânicas. No contexto biomédico, o polivinil álcool é vulgarmente utilizado como polímero-base para hidrogéis, conferindo boas propriedades mecânicas e de biocompatibilidade. Neste estudo foram utilizadas fibras de PVA (*Kuralon*^{TM} da *Kuraray*) de diâmetro micrométrico como reforço de cimentos de fosfato de cálcio para a avaliação das propriedades mecânicas dos cimentos, bem como a avaliação das propriedades químicas, estruturais e citotóxicas das fibras.

Com base nos resultados obtidos, melhorias significativas foram alcançadas nas propriedades mecânicas com a inclusão das fibras *Kuralon*^{TM} face aos cimentos desprovidos de fibras. *In vitro*, as fibras não revelaram ser citotóxicas para células percursoras de osteoblastos.

abstract

The development of bioceramics for regeneration of bone tissue has been widely explored as reflected by its high application frequency resulting from problems associated with congenital defects, bone diseases or trauma. In this context, since 1980 that calcium phosphate cements has played an important role as bone filler or as scaffolds for bone regeneration, presenting good properties in terms of biocompatibility and bioactivity. However, the mechanical properties of this class of bioceramics have limitations regarding to brittleness and low flexural strength. Thus, the areas of potential application of these cements are limited to non load bearing areas.

The cements reinforced with polymeric fibers, is a solution long been widely explored by civil engineering, in order to improve the mechanical properties of cements, increasing its toughness and ductility. From the same engineering principle, to reinforce composites for medical purposes, polymeric fibers made of natural and synthetic polymers have been studied. Promising results *in vitro* and *in vivo* have been achieved, but without translation towards applications in load bearing areas.

Polyvinyl alcohol fibers are used for the reinforcement of ceramic composites such as concrete because of their beneficial mechanical properties. In the biomedical context, polyvinyl alcohol fibers are commonly used as a polymer-base for hydrogels, offering good mechanical properties and biocompatibility. In this study was used microsized PVA fibers (*Kuralon*^{TM} from *Kuraray*) as reinforcement of calcium phosphate cements for the mechanical properties evaluation, as well as the analysis of the chemical, structural and cytotoxic properties of the fiber.

On basis of the results of this study, significant improvements were achieved in the mechanical properties with the inclusion of *Kuralon*^{TM} fibers compared to cement devoid of fiber. In vitro, the fibers were not cytotoxic to osteoblasts precursor cells.

acknowledgements

A lot of people helped me to establish this study. I want to thank all of them, because I would not be able to finish it without them.

First and foremost, I would like to thank all people of the Biomaterials department at the UMC St. Radboud University. I would like to thank my supervisor, Professor Sander Leeuwenburgh, for his guidance, support and teaching during my M.Sc. project. I would like to express my great appreciation to my co-supervisor, Sónia Schickert, for her kind guidance, patience and encouragement as well as thank her the warm welcome she had during my stay in The Netherlands. My word of gratitude to PhD students and technicians for the good moments and assistance and with whom I learned a lot. A special word to Mariateresa Brindisi, Alessandra Curci, António Castro, Nathan Kucko and Robin Abraham for the friendship and affection.

A special “thank you” to Ricardo Serôdio who was a real fellow at all times we spent at work and fun times, during the 6 months in Nijmegen and for all the help and support given during the accomplishment of this thesis.

I would like to thank the Professor Ana Leite Oliveira for the opportunity to go perform my thesis in the Netherlands and for all the support given during the accomplishment of this thesis.

My word of gratitude to the Escola Superior de Biotecnologia – Universidade Católica do Porto for all the support during my academic path.

To all my friends a word of thanks for being my refuge and a preponderant aid in the fight against all odds.

Finally, I would like to thank my family for their efforts, unconditional support and inspire me in all the moments, especially to my brother Tiago, for being an example and for their fundamental support in the realization of this thesis.

contents

list of figures

around the fiber. (G) - *Kuralon*™ fiber embedded in calcium phosphate. (H) - Non-sterilized *Kuralon*™ fiber incorporated in CPC matrix.

Figures 24 - µ-CT cross-section images. (A) control formulation; (B) 1.25 wt.% 3mm. (C) 1.25 wt.% 6mm formulation; (D) 2.5 wt.% 3mm formulation; (E) 2.5% 6mm formulation; (F) 5 wt.% 3mm formulation; (G) 5 wt.% 6mm formulation.

Figures 25 (A/B) - Three-dimensional µ -CT reconstruction images of 5 wt.% 6mm specimen with the air pocket and fibers hank highlighted in green and blue, respectively. (A) Transversal and longitudinal section. (B) Longitudinal section.

Figure 26 - DNA concentration of each fibers concentration in direct contact with M3CT3 cells at the different time points.

Figure 27 - DNA concentration of each fibers concentration in indirect contact with M3CT3 cells at the different time points.

list of tables

list of abreviations

ACP – Amorphous calcium phosphate
CaP – Calcium phosphate
CPC – Calcium phosphate cement
DNA – Deoxyribonucleic acid
dsDNA – Double-stranded deoxyribonucleic acid
ECC – Engineered cementitious composites
EDTA – Ethylenediaminetetraacetic acid
FBS – Fetal bovine serum
FRCPC – Fiber reinforced calcium phosphate cement
FTIR – Fourier transform infrared spectroscopy
GA – glutaraldehyde
ICP-OES – Inductively coupled plasma atomic emission spectroscopy
ITZ – Interfacial transition zone
L/P – liquid/powder
MW – molecular weight
PBS – Phosphate-buffered saline
PPB – Parts per billion
PPM – Parts per million
PVA – Polyvinyl alcohol
SEM – Scanning electron microscope
UV – Ultraviolet
WOF – Work of fracture
XRD – X-ray diffraction
α-MEM – Alpha minimum essential medium
α-TCP – Alpha tricalcium phosphate
μ-CT – Micro computed tomography

chapter 1
introduction

1.1 Bone

The human skeleton consists of more than 200 bones, a vital tissue that provides support, protection and shape to the human body[1,2]. Bone is a natural composite material, that consists about 60% (wt.) mineral, 30% (wt.) matrix and 10-20% (wt.) of water[3]. The organic matrix consists mostly of collagen, which is responsible for the resilience and tensile strength of bone. The mineral phase is composed of hydroxyapatite, a calcium apatite responsible for the unique mechanical performance. A schematic view of the composition of bone can be found on *Figure 1*.

Bone is a dynamic tissue that is naturally remodeled throughout life through biochemical processes. Bone-specific cells – osteocytes, osteoblasts, osteoclasts – and other cells - hematopoietic cells, mesenchymal cells and immune cells – work together in order to preserve the integrity, optimize the function and maintain integrity of bone. Specifically, osteoblasts and osteoclasts are involved in the processes of bone formation and resorption[3,4].

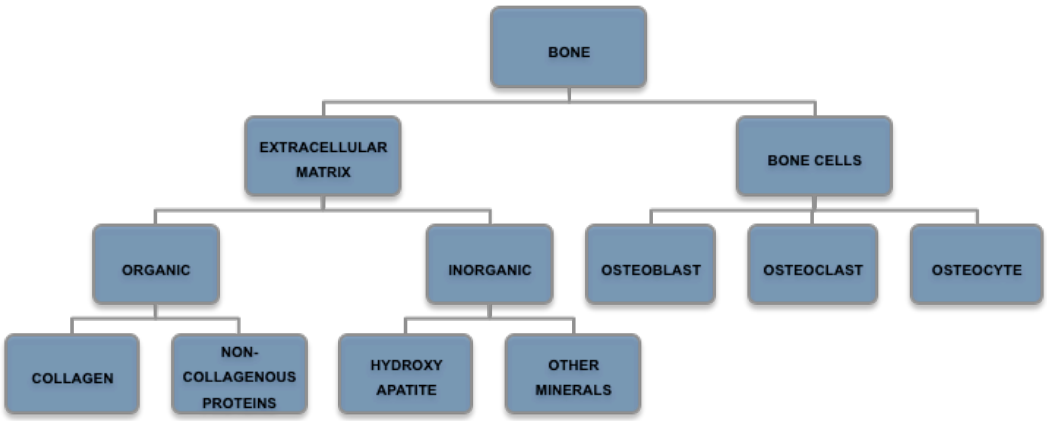

Figure 1 - Composition of bone[3,4].

1.2 Bone grafts

Bone is the second most transplanted tissue. Annually, 2.2 million bone grafting procedures are performed in the world to repair bone defects in orthopedics, neurosurgery and dentistry[5].

The ideal bone graft should be osteogenic, biocompatible, biodegradable, able to provide structural support, easy to use and cost-effective, which requires a set of specific features[6]. Osteogenesis, osteoinduction, and osteoconduction are the three essential elements of bone regeneration, regarding the final integration of the grafting material in the host bone, a process called osteointegration. The osteogenic potential of the graft consists in the ability of the cellular elements within a donor graft, proliferate and differentiate to osteoblasts and eventually to osteocytes. On the

other hand, osteoinduction is the stimulation and activation of host mesenchymal stem cells from the surrounding tissue, which differentiate into bone-forming osteoblasts; this process is boosted by the presence of growth factors within the graft, principally bone morphogenetic proteins (BMPs). Osteoconduction describes the facilitation and orientation of the bone matter into the bone scaffold to form bone[2,5,7,8].

The bone-grafting field resorts to autografts, allografts, xenografts and synthetic materials. Autografts, which are those whose the bone matter transplantation comes from the own patient, have the advantage of hosting living cells and growth factors. However this method holds several limitations, namely the lack of patient comfort, related with surgical procedures (it requires two operations) and the lack of availability of bone sources. Allografts and xenografts are grafting solutions extracted from another human being and from an individual of another species, respectively. Although these materials solve the problem of bone supply sources, there are some concerns regarding their biocompatibility of the grafts, raising concerns with immunological responses and diseases transmission.[8,9] Some structural and biological response characteristics of autografts and allografts are showed in *Table 1*, with particular emphasis for the natural high degree of compatibility of the autografts. Synthetic materials as metals, ceramics, polymers and cements are tested in order to be biomimetic, thus avoiding unwanted autoimmune responses and the common disadvantages that are constantly related to these surgical techniques[8]. Some synthetic bone graft approaches include the association of the material with the patient own cells as well as recombinant growth factors improving the bone regeneration allowing the development of a tissue similar to the original[9].

Table 1 - Autograft and allograft: structural and biological response characteristics[5].

GENERAL FEATURES / BONE GRAFT			Structural strength	Osteoconduction	Osteoinduction	Osteogenesis
Autograft	**Cancellous**		No	+++	+++	+++
	Cortical		+++	++	++	++
Allograft	**Cancellous**	Frozen	No	++	+	No
		Freeze-dried	No	++	+	No
	Cortical	Frozen	+++	+	No	No
		Freeze-dried	+	+	No	No

1.3 Calcium phosphate cements (CPCs)

Nowadays, a variety of bone-graft-substitute materials are currently commercially available for orthopedic and dental use (*Table 2*). From the economic point of view, bone filling materials have a high added value, thus high market potential[9]. In the period from 2001 to 2004, the number of bone

graft procedures tripled from half a million to 1,5 million and in 2013 the market expectations for tissue engineered products for musculoskeletal applications were around 39$ billion, just in USA[5,7]. Since LeGeros and his co-workers and Brown and Chow introduced calcium phosphate cements, their research interest never stopped growing[10,11].

Table 2 - Bone-graft-substitute materials.[5]

Type	Graft	Osteoconduction	Osteoinduction	Osteogenesis	Advantages
Bone	**Autograft**	3	2	2	"Gold standard"
	Allograft	3	1	0	Availability in many forms
Biomaterials	**DBM**	1	2	0	Supplies osteoinductive BMPs, bone graft extender
	Collagen	2	0	0	Good as delivery vehicle system
Ceramics	**TCP, hydroxyapatite**	1	0	0	Biocompatible
	Calcium phosphate cement (CPC)	1	0	0	Some initial structural support
Composite grafts	**β-TCP/BMA composite**	3	2	2	Ample supply
	BMP/synthetic composite	–	3	–	Potentially limitless supply

Score: 0 (none) to 3 (excellent); **DBM:** demineralised bone matrix; **TCP:** tricalcium phosphate; **BMA:** bone marrow aspirate; **BMP:** bone morphogenetic protein

Bioceramics are one of the most explored class of materials that interface with bone. Among these, calcium phosphates stand out as a material that has perhaps been studied most extensively, and they are available as allogenic, sintered or cementitious materials[12]. Calcium phosphate cements consist of a mixture between a liquid and solid phase, forming a paste which solidifies. The final product resulting from the chemical reaction, depends on the cement formulation method in terms of the kind of components used, the Ca/P ratio of the components and the liquid/powder ratio[13,14]. These materials have been extensively studied in the 1980s in the field of orthopedics, mainly as bone substitutes for the treatment of bone diseases (e.g. bone tumors), in the restoration after traumatic events (e.g. delayed unions, non-unions and malunions[5]) and congenital defects (e.g. achondroplasia, osteogenesis imperfecta, osteoporosis). The first commercial CPC products were introduced in 1995 for the treatment of maxillo-facial defects and deformities as well as for the treatment of fracture defects[10]. In the field of dentistry, however, these materials have already been

used as bone filler since 1920[14]. The handling properties of calcium phosphate cements, hence injectability, as well the self-setting *in situ*, represent attractive advantages from these materials from the clinical point of view[9].

Calcium phosphate cements are promising materials for bone-grafting procedures. Calcium phosphate cements are bioactive ceramics, since they are chemically similar to the mineral component of the bone, hydroxyapatite[12]. Their excellent behavior in physiological environment - biocompatibility, bioactivity and osteoconductivity - attracted great attention in biomaterials research[9,15,16]. Calcium phosphate cements brought new alternative treatments mainly for clinical applications such as vertebroplasty, arthroplasty, cranioplasty in the orthopedics field and furcal exposes, root sensivity, open root apices and endodontic obturation in dentistry[10,17]. However, calcium phosphate cements are limited to non-load bearing defects or pure compression loading areas, due their brittleness properties. Beyond this handicap, there are still some aspects to be improved, such as the control of the resorption rate and the enhancement of the osteogenic potencial[16]. In order to improve these drawbacks, a large variety of compositions have been investigated[9,12].

1.3.1 Properties of Calcium Phosphate Cements

Calcium phosphate cements can be divided into two groups based on their final products: apatite or brushite. Both are formed through a dissolution–reprecipitation process and can be obtained via an acid-base reaction or via a conversion reaction of a metastable compound, either α-tricalcium phosphate (α-TCP) or a so called amorphous calcium phosphate (ACP)[9]. The formation of these products relies on the environment pH. If pH>4.2 apatite shall be formed but if pH<4.2 brushite is formed[9,12]. A fundamental difference between the two is that water is not needed for the setting of apatite cements while the setting reaction of brushite is hydraulic, becomes soluble in physiological conditions, decreasing their mechanical properties[12,16]. As mentioned in the previous section, the components used in cement formulation have a great influence on the properties of the formed matrix[16]. This properties such as setting time, porosity or mechanical behaviour are revealed in the microstructure of the matrix formed[13].

In general, apatite cements are the preferred calcium phosphate cements matrix, due to their similarity with mammalian bone calcium phosphates[9]. Tricalcium phosphate ceramics are suitable because of their similar stoichiometry with the amorphous bone precursors, whereas hydroxyapatite has a stoichiometry similar to bone mineral[5].

1.3.2 Mechanical properties

The poor mechanical properties of CPCs are the main reason that limits their widespread clinical usage of these materials. More specifically, their brittleness and toughness do not meet the requirements to allow for application in load-bearing sites[9,12].

The mechanical behavior of calcium phosphate cements is strongly determined by the microstructure of the cement. Factors that influence the microstructure include the type of calcium

phosphate, the relative proportions of the reactants in the mixture, powder or liquid additives acting as accelerators or retarders, particle size, liquid/powder ratio and the cement cohesion achieved during the samples assembly as result of pressure applied[9,10]. Technological factors are also involved in the properties evaluation of calcium phosphate cements, such as the use of *Vicat* tests for setting time measurements, or the so-called *Brazilian* test for the determination of the diametral tensile strength, factors that influence microstructure features[9,10]. When the dissolution–reprecipitation reaction occurs, an apatite crystal network is formed. The conformation of the apatite crystals network will determine the microstructure of the cement[9].

Porosity plays a fundamental role in the biological properties of the cement. However, the presence of pores is generally detrimental to the mechanical properties[8,18]. To increase porosity, microparticles can be used as porogens. Through mechanical tests, finite-element methods and mathematical models it was confirmed that increasing porosity results in an increased brittleness of the matrix, reduced mechanical properties performance[18]. It is then essential to find a compromise between pore size and amount and mechanical properties. *Lopez-Heredia et al.*[18] used PLGA porogens into calcium phosphate cement with different sizes and amount, and recommended the use of porogens with a minimum size of 40 μm and incorporated at an amount of 30 wt. % as the optimum combination. The interconnectivity of the cements is also influenced by the amount, size, morphology and distribution of formed apatite crystals[18].

Although several studies have been performed to enhance the mechanical properties of the calcium phosphate cements, these still lack satisfactory mechanical behavior, with regard to flexural strength, fracture toughness and cyclical stresses[19]. The mechanical properties by themselves should be evaluated, according with the application site and the defects on the biomaterial processing (e.g. microstructure defects). Fracture toughness was described as the ability of a material containing cracks or notches to resist crack propagation that could be conditioned by the microstructure or some kind of reinforcement[9]. Because it is easy to calculate, it is a generally accepted procedure to use work of fracture instead of fracture toughness as a measure for the toughness of calcium phosphate cements, despite not being an intrinsic material property[12].

A comparison between the mechanical properties of cortical bone and calcium phosphate cements can be found on *Table 3*. Among the included mechanical properties, compressive strength values are very often used in literature as standard values to allow a comparison between different calcium phosphate cement formulations and bone. The compressive tests are easy to perform and therefore are taken as a measure of evaluation of the calcium phosphate cements mechanical properties. However, it should be emphasized that compressive strength alone is not enough to reach a conclusion regarding the mechanical properties of the materials. Additionally, compression values are also not enough to be used as a means of comparison between calcium phosphate cements and bone, since the *in vivo* situation includes not only compression stresses, but also other types of mechanical stresses such as tension, shear, bending and torsion[9].

Table 3 - Mechanical properties of cortical bone and CPCs[9,19].

MATERIAL / MECHANICAL PROPERTIES	Cortical bone	CPCs
Compressive strength (Mpa)	**130 - 180**	**0.2 - 184**
Flexural strength (Mpa)	**≈ 200**	**5 - 15**
Fracture toughness (Mpa/m^2)	**2 - 5**	**0.15 - 0.5**

As a basis of comparison when related to cortical bone, some calcium phosphate cements and cortical bone mechanical properties tested by some research groups, show that there is still much work to do with respect to the reliability of calcium phosphate cements mechanical properties.

At the early stage of bone regeneration, while bone modeling/remodeling is taking place, the bone substitute material should be able to sustain the mechanical stresses present in the implantation site. For this purpose, many strategies were followed, namely by densifying and homogenizing the cement matrix. In order to improve density, strategies such as compacting the paste in different axis to decrease the volume fraction of the pores and decreasing the liquid/powder ratio were reported[12,18]. For homogenizing the cement, the addition of small amounts of nitric acid, which improves the mixing, as well as sodium citrate, which avoids the agglomeration of the apatite particles is also reported[9]. In 2012, Liu *et al.*[20] demonstrated that the incorporation of cellulose ether additives increased the tensile and flexural strength, as well as the fracture toughness significantly.

1.4 Fiber reinforced calcium phosphate cements (FRCPCs)

For more than 3500 years, fibers have been used to reinforce cement matrices in the field of civil engineering[21]. First, fibers with natural origin as straw and horse-hair were dispersed in cement-based materials, aiming to decrease the typical brittleness of the cement[21,22,23]. Until today and due to the powerful civil construction economy, a number of techniques and technologies have been used aiming the so-called high performance concrete[22]. Based on the strategy used by civil engineering, the biomedical field also started in the early 1980s to reinforce calcium phosphate cements with polymeric fibers, but only reported in 2000s[19].

The reinforcement of cements with fibers gives origin to three phenomena: fiber bridging, crack deflection and frictional sliding (*Figure 2*)[9]. Fibers act as an aid on keeping the consistency of the matrix in nano/microcracking propagation, resistance in tension, shear and bending, ductility, and energy absorption capacity. When the matrix starts to crack, the fibers bridge the crack to resist its further opening and propagation. Consequently, crack deflection by the fibers prolongs the distance over which the crack propagates (change in the direction of the crack propagation), consuming more energy in newly formed surfaces. Finally, fibers decrease the propagation velocity of the cracks and

consume part of the energy applied in the matrix avoiding the critical failure of the cement and absorbing the energy related with the frictional sliding of fibers against the matrix during pullout, mainly due do to shear stresses[12]. Fiber bridging and crack deflection have been reported[9] as the major contributors to the fracture toughness of human bone, consisting of hard mineral nano-particles (carbonated apatite) and a fibrous polymer (collagen)[9].

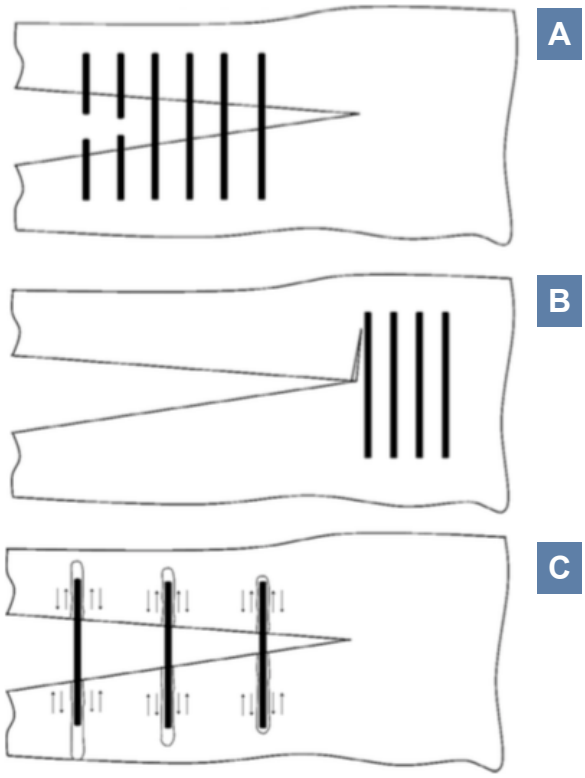

Figure 2 – Phenomena that occur in fiber reinforced cements: (A) fiber bridging,(B) crack deflection and (C) frictional sliding[9].

The selection of fiber material is essential for fiber reinforced calcium phosphate cements composites. Since these fibers are intended for biomedical applications, they have to be biocompatible. Additionally, ideal bone substitutes should degrade completely, in such a way that allows for a complete replacement of the material for newly formed native bone. For this purpose, the fibers should also be biodegradable. To date, several types of polymeric fibers have been tested as reinforcing agents for calcium phosphate cements. Fibers from natural origin, such as silk, wool, hair, seed of asbestos, and from synthetic origin, such as steel, titanium, polyamide, polyurethane, carbon or glass have been reported to be selected[19,24]. In addition to the type of fiber, fiber parameters should such as fiber length, fiber diameter, volume fraction, fiber orientation and fiber/matrix adhesion also influence the composite properties[19,24].

Experimental animal assays have been performed with different types of fiber reinforced calcium phosphate cements. Fiber degradation behavior was tested in rabbits with hydroxyapatite based FRCPCs reinforced with PLGA fibers. Some undesirable results in terms of cytotoxicity and resorption of FRCPC in comparison with unreinforced CPC, however with better osteoconduction and degradability[12]. Other study performed in fractured canine radius with the implantation of FRCPC (HA

reinforced by collagen coated chitosan fibers), regarding the evaluation of the mechanical properties, showed better load bearing capability than the CPC control samples (*Figure 3*)[12].

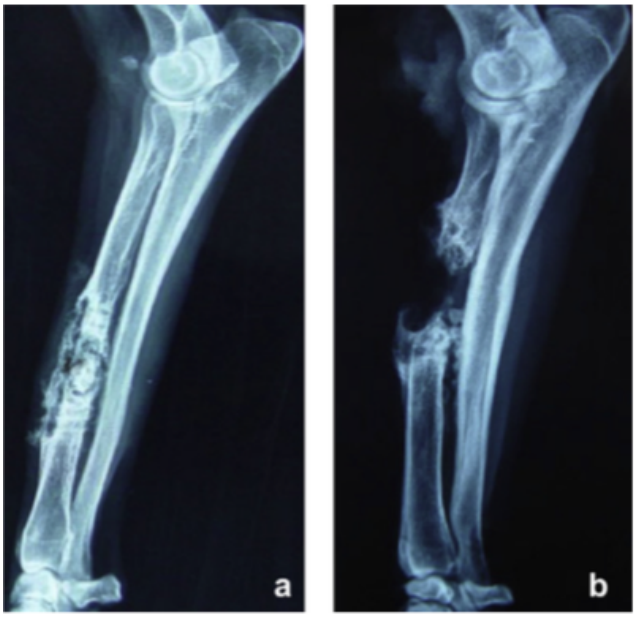

Figure 3 – Canine radius radiographic observation after 20 weeks in vivo. (a) FRCPC implant; (b) unreinforced CPC implant[12].

1.4.1 Characteristics of the fibers used for reinforcement

Fiber length and the quantity added to the cement matrix are parameters that highly influence reinforced cements. *Xu et al.*[24] demonstrated that the increase of these two factors generally improve the flexural strength, flexural modulus and work of fracture of the cements by increasing the fibers volume fraction from 0 to 10% and fiber length from 1 to 1000 mm with aramid, carbon, e-glass and polyglactin fibers. To evaluate the mechanical properties, the author fixed the fiber length in 75 mm varying the fiber volume fraction and fixed the fiber volume fraction in 5.7% varying the fiber length, in the aforementioned intervals. For example for polyglactin, the author observe an increase of ~ 20 MPa (from 10 to 30 MPa) with the increase of fiber volume fraction and an increase ~ 10 MPa (from 15 to 25 MPa) with the fiber length variation for flexural strength. For flexural modulus an increase of ~ 2 GPa (from 2 to 4 GPa) when varied the fiber volume fraction and no differences with the increase of fiber length. The work of fracture, increased ~ 3 kJ/m^2 (from 2 to 5 kJ/m^2) with the increase of fiber volume fraction and the same increase for fiber length till ~ 50 mm, followed by a decrease. However, the addition of fiber content in calcium phosphate paste is limited by the resulting workability[25,11]. According with *Buchanan et al.* [11] the workability of the cement is committed for fiber volume fractions of 5% and above and additional liquid is required for fiber volume fractions of 14% and above. The fiber length has an important purpose in the control opening and propagation of crack[21]. Brandt[21] observed that short fibers are more properly to control microcracks once they are more dispersed in cement matrix and long fiber to control larger cracks (*Figure 4*).

Figure 4 – Role of short and long fibers during the cracking process[21].

Fiber distribution plays a fundamental role for the mechanical properties of the composite cement[26]. The aggregation of fibers resulting from the high fiber aspect/ratio, is not only a problem of processing but also results in poor mechanical properties due to inhomogeneities[12]. Good dispersion allows a more uniform stress distribution and minimizes the appearance of stress-concentration points. A random orientation of fibers results in lower efficiency of reinforcement than does perfect alignment, however perfect alignment generates anisotropy in the mechanical properties, which is not favorable for cyclic forces[26]. According to Pinho *et al.*[26] fiber alignment in the matrix allows a lower amount of fiber content to achieve the same mechanical behaviour than with a randomly dispersion. Several algorithms and computer models are being developed in order to enhance the fiber dispersion[27,28]. A homogeneous distribution of the fibers in the matrix could be influenced by the fiber diameter as well as its interaction with the composite[12]. Nanofibers are most likely to aggregate due to their high specific surface, what inhibits a successful dispersion of the fibers. Several equations[28] provide us an estimate of the critical fiber volume content as a function of the mechanical properties of the fiber and the matrix.

For an efficient strengthening effect provided by the fibers when the composite is subjected to a load, the fiber/matrix interaction should be optimal as possible: on the one hand, the interaction should not be too strong to avoid the possibility of a premature fiber fracture and on the other hand, the interaction can't be too weak to compromise energy dissipation due to weak fiber pullout forces. The zone where the fiber/matrix interaction occurs is called "interfacial transition zone" (ITZ)[12]. The ITZ is a thin layer (5 to100 μm) closely related with the surface properties (roughness) and the shape (kinked or crimpled shape, dog bone shape or with beads at the fibers ends) of the fiber[12]. In order to increase the affinity between the fibers and the matrix, several methods have been developed. Valadez-Gonzalez *et al.*[29] tested treatment of the fibers surface in different ways: with chemical solutions – alkaline and silane – and with a preimpregnation with polyethylene dilute solution, observed an improvement of shear strength by morphological modification of the fiber surface. The alkaline solution increased the fiber surface roughness and increments the exposure of few reactive groups, while the silane-coupled agent increased the fiber-matrix adhesion. The fiber preimpregnation allowed a better fiber wetting, enhances the mechanical interlocking between fiber and matrix[29]. Plasma surface treatments, aim change the polarity and the creation of patterns on the surfaces producing considerable differences in the load required for debonding of the fibers[30,31].

In order to obtain mechanically sustainable composites, it is important to be careful in the choice of each component – powder, liquid and fiber – which is added to the mixture in the assembly of the cement as well as the achievement of a homogeneous fiber distribution. The *Table 4* shows the set of criteria that must be taken into account for the processing and composite design of FRCPCs.

Table 4 – Parameters describing the processing and composite design of FRCPC[12].

CRITERION	FEATURES
Macrostructure	Short or long fibers
	Individual or woven fibers
	Macroporous or not
	Layered or homogeneous
	Isotropic or anisotropic
Fiber diameter	Macro, micro or nano fibers
Composition	Type of CPC
	Type of fiber
	Fiber content
	Fiber coating
	Matrix additives
Resorbability	Degradable or non-degradable
Functionalization	Drug delivery
	Cellularization
	Injectability

1.5 Polyvinyl alcohol (PVA) fibers

Polyvinyl alcohol is an organic synthetic polymer obtained from polyvinyl acetate by successive hydroxylation processes (*Figure 5*). Hydroxylation processes are responsible for adding the hydroxyl groups, which remove the acetate groups. Depending on the amount of acetate groups present in the backbone, PVA is divided in two groups: partly hydrolyzed or fully hydrolyzed[32]. The hydrolysis degree has a strong influence on the physical, chemical and mechanical properties of the PVA[33,34]. Hydroxylation and polymerization provide PVA with improved mechanical properties due to the improved chemical stability[34]. The macromolecule is hydrophilic consequently, soluble in water[34]. However as the degree of hydroxylation and polymerization increase the solubility decreases and the crystallization becomes more difficult[33].

Moreover, for the use in biomedical applications, PVA needs to be crosslinked in order to improve it mechanical properties and thermal stability, related with the water quantity uptake. Thus PVA can be more stable in physiological environment and its range of application broadens[34].

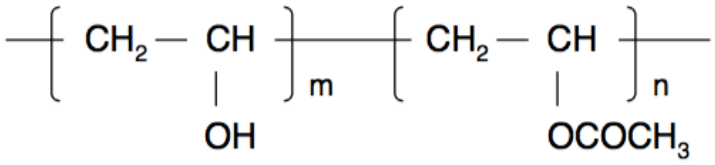

Figure 5 – PVA chemical structure.

1.5.1 PVA as reinforcement phase of cementitious matrices

PVA fibers started to be used in reinforced engineered cementitious composites in civil engineering as they are considered highly suitable for reinforcement of concrete. Tadavarthy *et al.* [35] use PVA for biomedical applications for the first time in 1975. The author implanted PVA hydrogels subcutaneously and intramuscularly into rabbits. No adverse biological responses were observed in the surrounding tissue, although the hydrogel poor mechanical and water-retention properties have prevented the development[33,36]. From then, PVA was used in different forms such as particles for vein embolization[33] and incorporated in cement matrix for scaffolds in tissue engineering[33]. Several *in vitro* and *in vivo* tests related with their bioadhesive characteristics, water absorption abilities and low toxicity in some medical devices as contact lenses and nerve guides were performed. These studies suggested that PVA is stable and safe to use for medical devices[33].

Studies have shown that PVA applied in different forms (implantable or non-implantable devices) can provide desirable biomimetic behaviour regarding low protein adsorption characteristics, biocompatibility, high water solubility, and chemical resistance[33].

The manufacturing process determines the biomechanical performance such as the thawing and freezing protocol, the addition of saline and crosslinking density[33]. In terms of mechanical properties, crosslinked PVA fibers have a Young's modulus of 39 GPa and a tensile strength of 1.6 GPa (*Kuralon*^{TM} from *Kuraray*). When compared to other fibers used in reinforcement of CPCs, PVA shows superior mechanical properties[37]. For example, *Vicryl*^{TM} 910 has a Young's modulus of 0.3 GPa and a tensile strength between 0.46 and 0.51 GPa[12].

1.5.2 *Kuralon*^{TM}

Kuralon^{TM} is the brand name given by *Kuraray* to one of their commercially available type of PVA fibers. *Kuraray* is one of the largest suppliers of synthetic microfibers, an international leader in the development and use of innovative high-performance materials and the leading producer of polyvinyl alcohol fibers. The *Kuralon*^{TM} fibers are classified as fibers for several industrial applications among them the reinforcement in construction industry for cements and concretes. Some special features are highlighted such as the high tenacity and Young modulus, low elongation, creep and heat shrinkage in hot air, chemical resistance, affinity to rubber and resins, UV stability and hydrophilic character *(Figure 6)*.

Kuralon^{TM} fibers are produced in a specific way described vacantly by *Kuraray*. Low molecular weight polyvinyl alcohol is dissolved in water and wet spun into an aqueous salt bath. The resulting yarn is stretched and heat treated and submitted to a crosslinking process based on 2 steps: the first

one, the yarn is placed in a monoaldehyde (e.g. formaldehyde or benzaldehyde 50-100g/L) or dialdehyde (e.g. linear compounds such as glutaraldehyde (GA) and hexane-1,6-dial, aromatic compounds such as orthophthalaldehyde, isophthalaldehyde or using like the combination of 2 or more) bath at 70-90^{o}C to promote the intramolecular bonds and the second one, a mixed solution of monoaldehyde and acid, acting as reaction catalyst (e.g. sulfuric acid 30-150 g/L) will promote the intermolecular connections[38].

Figure 6 - Kuralon™ PVA fibers.

1.6 Aim and hypothesis of this thesis

Currently, no tough and strong osteoinductive cements are available for treatment of bone tissue defects in load bearing areas. There are many health problems associated with bone wear in these regions. Consequently, major concerns at public health level and high costs in the treatment of the patients (due to the large number of bone graft procedures) arise. Calcium phosphate cements have been reinforced with fibers to solve this problem, but the efficiency of fiber reinforcement of calcium phosphate cements is not optimal yet. PVA fibers are currently used in cement reinforcement strategies in civil engineering but are not commonly used in calcium phosphate cements for biomedical engineering purposes. Therefore, the following work aims to understand if it is possible to improve the strength and toughness of calcium phosphates cements by incorporation of commercially available polyvinyl alcohol fibers (PVA, Kuralon™, 26μm in diameter and 6mm in length). In addition, the cytotoxic properties of these fibers will be evaluated in order to assess their feasibility for future clinical use. Our hypothesis were that I) the increase of the weight percentage and length of *Kuralon*™ PVA fibers into calcium phosphate cements increase its mechanical properties in terms of flexural strength, flexural modulus and work of fracture and II) the viability and proliferation of cells decreases with the increase of the amount of *Kuralon*™ PVA fibers.

Research question

Can polyvinyl alcohol fibers (Kuralon^{TM}) be used to reinforce CPCs in terms of mechanical strength and toughness?

chapter 2
materials and methods

In the present work, calcium phosphate cements reinforced with *Kuralon*^{TM} PVA fibers were produced by a combination of α-tricalcium phosphate powder mixed with a 4% sodium phosphate aqueous solution, to generate hydroxyapatite as an end-product. Cements with increasing fiber content (1.25%, 2.5% and 5% w/w) and different fiber lengths (3mm and 6mm) were developed and characterized.

Given the unknown chemical properties of the *Kuralon*^{TM} PVA fibers, chemical and structural analyses were performed using Fourier transform infrared spectroscopy (FTIR), X-ray diffraction (XRD) and inductively coupled plasma-optical emission spectroscopy (ICP-OES) analysis. The cytotoxicity of the fibres was tested using indirect and direct contact assays using a M3CT3 cell line. After incorporation of the fibers into the calcium phosphate matrix, the FRCPC mechanical properties of the samples were also evaluated using a three point bending test following SEM and μ-computed tomography (μ-CT) analysis to observe the microstructure of materials after cracking and to evaluate the fiber/matrix interactions.

2.1 Materials

All the materials and reagents used for this study are as follows:

Elastosil RT 601A (purchased from *Wacker* (Munich, Germany) and Elastosil RT 601B (purchased from *Wacker* (Munich, Germany) were used for the molds preparation. α-tricalcium phosphate powder (α-TCP) from *CAM Bioceramics* and sodium phosphate 96% (purchased from *Sigma-Aldrich*) were used as matrices. Commercial PVA *Kuralon*^{TM} were provided by *Kuraray* and used to reinforce the calcium phosphate cements and to chemical, structural and biological characterization. 99% hydrolysed PVA powder (MW=133000g/mol, purchased from *Polysciences*) was used to FTIR and XRD. Phosphate buffered saline (PBS) (purchased from *Gibco*), α-MEM (without ascorbic acid, purchased from *Gibco*) and Gentamicin (500mg/mL, purchased from *Gibco*) were used to the cytotoxicity assay.

2.2 Methods

I) Silicone moulds

The silicone molds (*Figure 7*) were used for the preparation of calcium phosphate cement bars for further characterization. An Elastosil RT 601A solution with 1% of Elastosil RT 601B was prepared.

This solution was stirred vigorously (vortex and stirring rod) and centrifuge at 5000 rpm for 5 minutes at room temperature, to remove the air bubbles. The solution was placed in a Petri dish with the teflon bars and the remaining air bubbles were removed with a vacuum pump. The molds were dried during 4 hours at 60^{o}C in an oven and then removed from the Petri dishes.

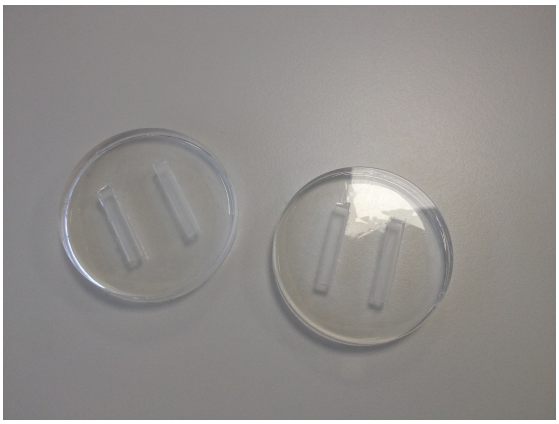

Figure 7 - Silicone molds. Used as model for preparation of FRCPC's samples.

II) FRCPC's samples

Cements with different fiber content (1.25%, 2.5% and 5% w/w) and fiber lengths (3mm and 6mm) were developed and characterized. The *Kuralon*^{TM} PVA fibers with 26 microns of diameter were used in two lengths, 3mm and 6mm. The weight content of fibers were based on experimental assays, and 5 wt% was observed to be the maximum fiber amount based on the handling properties of the resulting cements.

The *Kuralon*^{TM} PVA fibers were mixed with the 4% sodium phosphate aqueous solution and then added to the calcium phosphate powder. The paste was mixed with a metallic spatula during 30-45 seconds and placed in silicone molds to get a parallelepiped shape with the dimensions of 4 x 4 x 25 mm^3 (*Figure 8*).

The formulations with bigger amount of fibers naturally revealed more difficulties in handling, and in obtaining a good dispersion of fibers in the matrix. The 3mm fibers showed more miscibility in comparison with 6mm length fibers. The production process of the samples, related with the placement of the paste in the silicone molds, proved to be inefficient from the point of view of getting a homogenous mixture. It was difficult to avoid air bubbles.

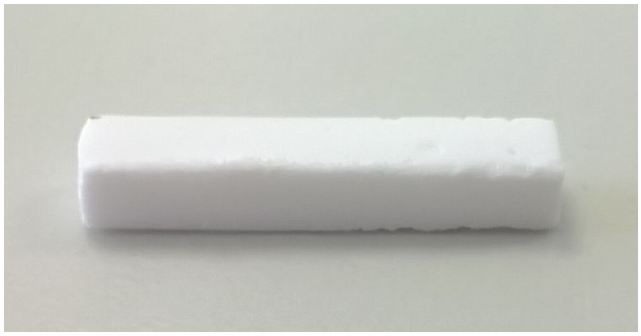

Figure 8 - Parallelepiped shape FRCPC specimen.

2.2 *Kuralon*™ PVA fibers

For comparative purposes in terms of chemical and structural composition was used a 99% hydrolysed PVA powder, with a 133000g/mol of molecular weight, in an attempt to better understand *Kuralon*™ PVA fibers. In the *Kuraray* patent, the fiber production process is poorly described, however it is referred that the degree of polymerization of the PVA used is not specifically restricted, but it is the higher the better to produce the desired reinforcement effect, having been chosen the PVA powder refered above.

2.2.1 Fourrier Transform Infrared Spectroscopy (FTIR)

Fourier transform infrared spectroscopy (FT-IR, UATR Two, PerkinElmer, USA) was used to identify the molecular structure of *Kuralon*™ fibers in comparison to other commercial PVA (99% hydrolysed PVA powder, MW=133000g/mol, *Polysciences*). FTIR spectra were obtained in the range of wavenumber from 4000 to 400 cm^{-1} during 5 scans, with 4 cm^{-1} resolution. PVA powder was grinded with a mortar, in order to obtained finer grains. The FTIR spectra were normalized and major vibration bands were associated with chemical groups. To minimize the interferences the spectra were smoothed.

2.2.2 X-Ray Diffraction (XRD)

The XRD patterns of the *Kuralon*™ PVA fibers and pure PVA powder 99% hydrolyzed were collected on a theta-2theta PANalytical X'Pert-3 (Almelo, the Netherlands) diffractometer. The instrument was scanned over a 10°- 30° 2θ with a 0,0050° step size and a counting time of 1,00s for a total measurement time of $\approx$ 1h. A fibers flat sample with 1mm of height was made recurring to a hydraulic press due to difficulties to reduce the PVA fibers to powder. Were used 1/16° receiving slits for both samples (powder and flat sample). The instrument was run at 45 kV and 40 mA.

2.2.3 Inductively Coupled Plasma Optical Emission Spectrometry (ICP-OES)

The elemental composition of the PVA fibers was analyzed using inductively coupled plasma optical emission spectrometry (ICP-OES). The presence of 41 elements in the samples was analyzed. To this end, the *Kuralon*™ fibers were first dissolved in 10%(v/v) nitric acid at a concentration of 0,2% (m/v) prior to ICP analysis. The salt concentration for the ICP-OES analysis was lower than 0,2%.

In order to investigate the presence of elements comparatively with the typical composition of PVA, and to complement the chemical analysis of the *Kuralon*™ PVA fibers, a element scan was carried out through an ICP analysis.

2.2.4 Scanning Electron Microscopy (SEM)

SEM analysis was performed on the *Kuralon*^{TM} PVA fibers, using a Zeiss Sigma 300 (Oberkochen, Germany) scanning electron microscope (SEM) after being sputter coated with chromium. The fibers were analyzed at different magnifications ranging between x600 and x5,6k, with an acceleration voltage of 7.00kV. *Kuralon*^{TM} fibers were sterilized under UV radiation and with argon plasma treatment to compare with and unsterilized *Kuralon*^{TM} fibers and analyzed the modifications caused in the fibers surface.

2.3 Fiber Reinforced Calcium Phosphate Cements (FRCPCs)

The samples were kept in the molds under a 50N force (approx.) applied using glass slides. Afterwards, the bars were submerged in PBS during 3 days in an incubator at 37^{o}C in dynamic conditions at 20 rpm.

10 samples of each formulation were prepared in addition to a control group without fibers. The composition of the various experimental groups is provided in the *Table 5*.

Table 5 - Composition of the different CPC's samples. This procedure was done for 3mm and 6mm fiber length.

CONTENT / SAMPLES		α Tricalcium phosphate cement (g)	Kuralon^{TM} fibers (g)	4% sodium phosphate aqueous solution (µl)
Fiber weight content (wt.%)	Control	1,5000	0,0000	750,00
	1,25	1,4925	0,0075	750,00
	2,5	1,4850	0,0150	750,00
	5	1,4700	0,0300	750,00

2.3.1 Three point bending tests

The mechanical tests of the FRCPCs samples were performed on a tensile testing machine (MTS, 858 MINIBionixII) computer controlled (*Figure 9*).

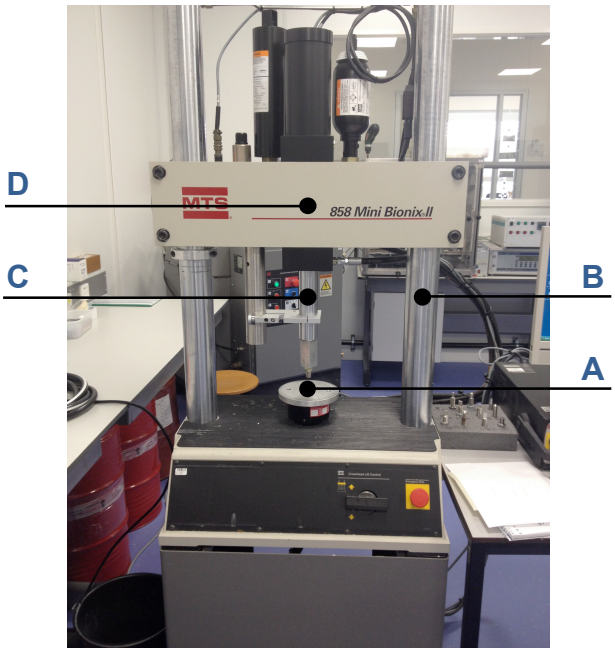

Figure 9 - Three point bending device. (A) displacement sensor; (B) guiding rods; (C) loading force bar; (D) falling crosshead.

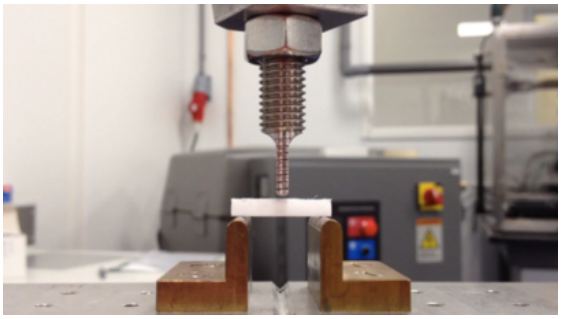

Figure 10 - Positioning of a specimen on 3 point bending machine.

The samples were removed from the PBS and were dried with tissue papers by capillarity and placed on the supports as show in *Figure 10*. Load-displacement curves were recorded using *TestWorks4* software.

A standard three-point flexural test was used to fracture the specimens at a crosshead speed of 1,0 mm/min with a loading force bar with a width of 3mm (*Figure11)*.

Figure 11 - Loading force bar used in the test.

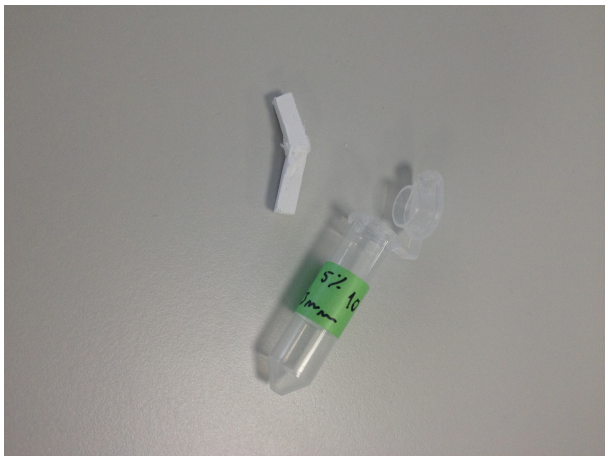

Figure 12 - Fractured FRCPC specimen (5% 3mm formulation) after 3 point bending test.

The samples (*Figure 12*) were placed on the support span of the load cell. Before testing, the dimensions of the bars were measured (thickness and width) to insert in *Testworks4* software.

Three point bending test was performed in order to obtain several FRCPCs mechanical properties, however due to samples heterogeneity in terms of shape and fibers content (amount and length) different parameters were settled down. For each formulation the test was stopped when the sample load resistance or the crack extension reached values considered reasonable for the analysis of desired mechanical properties.

The mechanical properties were evaluated from the load-displacement curve equation:

- Flexural Strength (S_c):

$$Sc = \frac{3 \times F \times L}{2 \times b \times h^2} \quad (2.1)$$

F – Maximum load at fracture point (N)
L – Length of support span (mm)
b – Width of specimen (mm)
h – Height/thickness of specimen (mm)

- Flexural Modulus (E_{bend}):

$$Ebend = \frac{m \times L^3}{4 \times b \times h^3} \quad (2.2)$$

m – Slope of trend line
L – Length of support span (mm)
b – Width of specimen (mm)
h – Height/thickness of specimen (mm)

- Work of fracture (WOF):

$$WOF = \frac{A}{b \times h} \quad (2.3)$$

A – Area under load-extension curve (N/m)
b – Width of specimen (mm)
h – Height/thickness of specimen (mm)

Each measurement was performed until the remaining force was less than 5N. The gage adjustment pre-load setting used was 0,5N to avoid that load data were not recorded below this value. Ten specimens were tested for each formulation.

2.3.2 Scanning Electron Microscopy (SEM)

SEM analysis was performed for the FRCPCs. The samples were evaluated using Zeiss Sigma 300 (Oberkochen, Germany) and Hitachi TM3000 (Tokyo, Japan) scanning electron microscope (SEM) after being sputter coated with chromium. The 5 wt.% fiber content samples were analysed at different magnifications (x50, x100, x500 and x1,0k). Were analyzed the FRCPCs bars after 3 point bending test.

SEM was used to observe the longitudinal cross-sections of the specimens after the mechanical test. The orientation of the fibers, crack propagation and pullout of fibers was examined in the cross-section of the FRCPC's specimens after mechanical tests.

2.3.3 Micro Computed Tomography (μ-CT)

To visualize the fiber distribution and porous structure within the CPC, the samples were scanned using micro computed tomography (μ-CT) equipment (Skyscan 1072, Aartselaar, Belgium). To the acquisition of the images were used a magnification of x40 at a resolution of 7.08 μm per pixel, with source conditions of 100 kV, 98 μA, rotation angle of 180° and rotation step of 0.9000°. Were used the FRCPCs bars after 3 point bending test.

2.4 *Kuralon*™ cytotoxicity assay: direct and indirect contact

In order to evaluate the fibers biocompatibility, the selected cells for the cytotoxicity assay were MC3T3, a osteoblastic cell line from *Mus Musculus* (mouse). MC3T3 were cultured for 10 days in alpha MEM medium supplemented with 10% v/v fetal bovine serum (FBS) at 37 °C, 95% relative humidity and 5% CO2. The medium was refreshed after every 3 days of culture. At 70-80% of confluence, cells were washed with PBS, detached using Trypsin/EDTA (0.25% w/v trypsin/0.02% EDTA) for 2 min, resuspended in Alpha MEM medium with 10% v/v FBS and then seeded with a density of 15.000 cells/cm².

The cytotoxicity of *Kuralon*™ fibers was determinated by subjecting the cells to a direct and indirect contact with the fibers. In the indirect method, the fibers were in contact with the medium in a incubator during 7 days. Cells were cultured for 24h, 48h, 72h and 7 days. At the selected time points, the culture process was stopped and the amount of DNA present in the wells was assesed through a QuantifluorTM dsDNA method.

For this assay the M3CT3 cells were cultured in medium composed of α-*MEM* (without ascorbic acid), 10% of FBS and 1% of gentamicin. Both methods started at the same time, however

the fibers to the indirect method were placed 7 days before in medium to let the fibers in contact with medium.

The well plates were left in the incubator according with the time points: 24h, 48h, 72h and 7 days. After each time point, the medium was removed and each well washed with PBS 2 times. 1mL of milliQ was added in each well and the plate placed in the freezer at -20°C. 2 cycles of freeze-thaw was done promoted the lysis of the cell membrane and the release of its DNA content. The cells and the medium were placed in a 24 well plate according with to *Figure 13*.

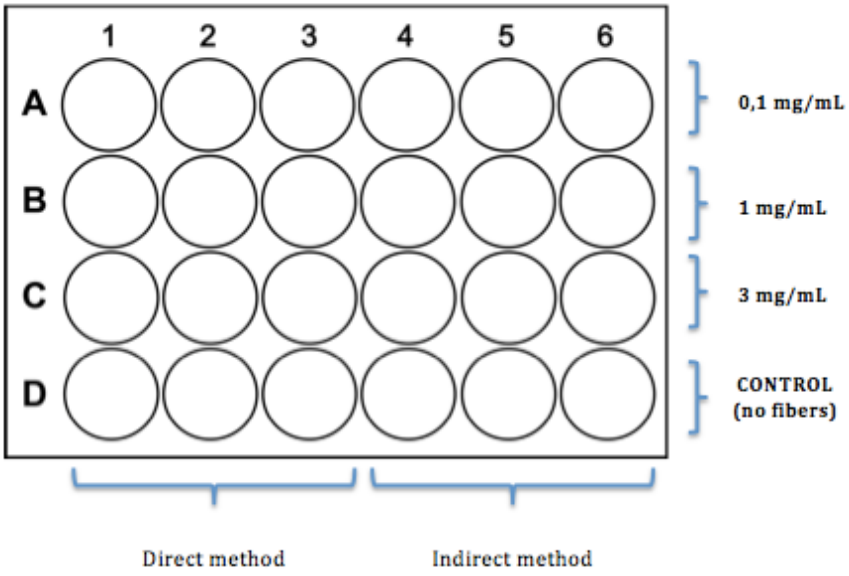

Figure 13 - Scheme of the 24 well plate with respective position for each method and concentration.

The well plates were read in a spectrophotometer (*Synergy HTX*, by *Biotek*), with excitation of 485/20 from tungsten light source at an emission of 528/20 nm. The data was analyzed with *Gen5* version 2.06 software. The fluorescence results obtained was converted in DNA concentration values through the linear equation given from the calibration curve. The DNA concentration data was used to evaluate the *Kuralon*^{TM} fibers cytotoxicity.

2.5 Statistical analysis

The statistical analysis was performed using *IBM SPSS Statistics 22* software.

Regarding the mechanical tests with the FRCPCs, differences between the amount of fibers (control, 1.25, 2.5, 5 wt.%), length of the fibers (3mm and 6mm), and the relationship between both groups were analyzed using a analysis of variance (ANOVA Two-way, Bonferroni).

Regarding the cell test, it was used a One-Way ANOVA (LSD) analysis, in order to investigate the existence of differences relatively to the cytotoxicity of the fibers in function of the different fiber concentration, considering, as the dependent variable, the concentration of DNA, and, as the independent variable, the fiber concentration.

In both studies, a 95% confidence interval was used, so the results were considered as statistically significant when p-value < 5%.

chapter 3
results

3.1 *Kuralon*™ PVA fibers

3.1.1 Fourrier Transform Infrared Spectroscopy (FTIR)

Figure 14 shows the FTIR spectra of *Kuralon*™ fibers and 99% hydrolysed PVA powder. Regarding the *Kuralon*™ fibers (red line), the large band observed between 3500 and 3200 cm^{-1} is related with the stretching O-H from the intermolecular and intramolecular hydrogen bond[39]. The vibrational bands observed 2840-3000 $cm^{-1,}$ can be related with the crosslinking process, revealing the more intensity linked to the stretching C-H from aldehydes groups, a duplet absorption peaks attributed to the alkyl chain. The intensity of the 1750–1735 cm^{-1} is weak due the high degree of hydrolysis, indicating that only few acetate groups are present in the polymer chain[39]. The peak at 1460 cm^{-1} is a bending vibration of C-H. The strong stretch 1000-1320 cm^{-1} is related with the link C-O[39]. The 99% hydrolysed PVA powder spectra (blue line) looks very similar with the *Kuralon*™ fibers spectra. The difference in the peaks highlighted can be related with the effect of crosslinking agent used for the crosslinking.

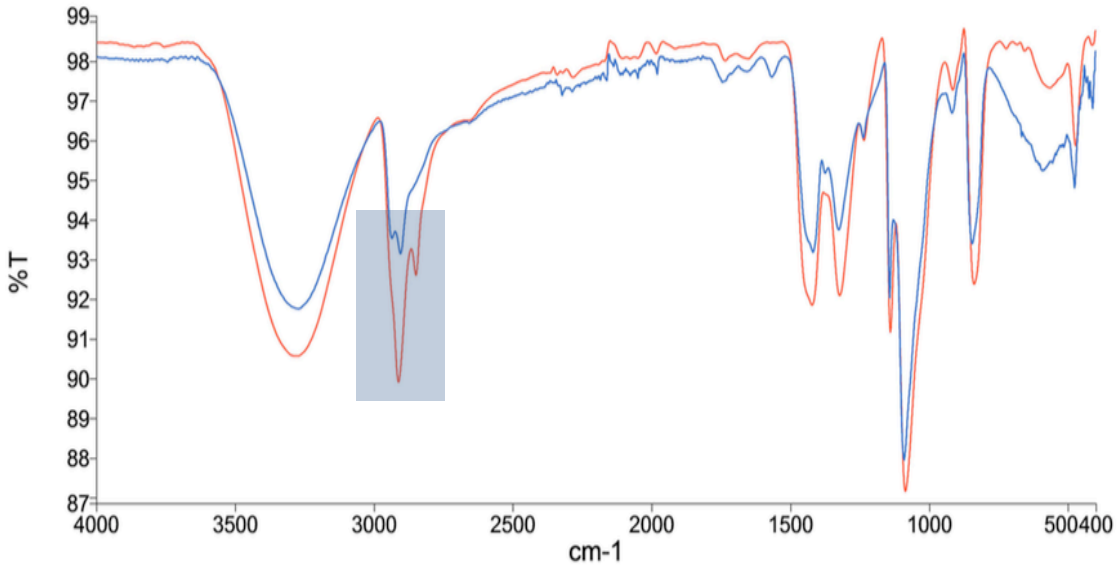

Figure 14 - FTIR spectra from Kuralon™ *fibers (red line) and 99% hydrolysed PVA powder (blue line).*

Table 6 shows the most characteristic band frequencies of PVA. The ranges for the absorption peaks vary according to the preparation method of the polymer. Factors such as the degree of hydrolysis and the amount of crosslinking agent has influence on the polymer chain structure.

Table 6 - General vibration modes and band frequencies of PVA[39].

Chemical group	Vibration mode	Wavenumber (cm-1)	Observation
O-H	Stretch	3550-3200	Intermolecular and intramolecular hydrogen bonds
C-H	Stretch	2840-3000	Alkyl groups
C-O	Stretch	1750-1735	–
C-O	Stretch	1141	Crystallinity
C-O-C	Stretch	1150-1085	–
H-C-H	Bend	1461-1417	–

Glutaraldehyde (GA) can be a dialdehyde used as a crosslinking agent, referred in the *Kuraray* patent specifications as a possibility. In the *Table 7* are presented the most characteristic bands of PVA crosslinked with GA.

Table 7 - General vibration modes and band frequencies of PVA crosslinked with GA[39].

Chemical group	Vibration mode	Wavenumber (cm-1)	Observation
O-H	Stretch	3550-3200	Intermolecular and intramolecular hydrogen bonds
C-H	Stretch	Two peaks in 2830-2695	Aldehyde
C=O	Stretch	1750-1735	–
C-O-C	Stretch	1150-1085	–

3.1.2 X-Ray Diffraction (XRD)

In order to investigate the degree of crystallinity of the *Kuralon*^{TM} PVA fibers, a comparison with a 99% hydrolysed PVA powder was performed, once its chemical composition was inconclusive by using FTIR analysis.

In *Figure 15* two clear peaks can be observed for both samples, around 19,5° and 22,5°. For both samples, both reflection peaks reveal high intensity *Kuralon*^{TM} fibers pattern, which can mean a

superior degree of crystallinity in comparison with the 99% hydrolyzed PVA. The peaks are broad, showing the semi crystalline character typical from the PVA, consistent with earlier studies (*Figure 16*).

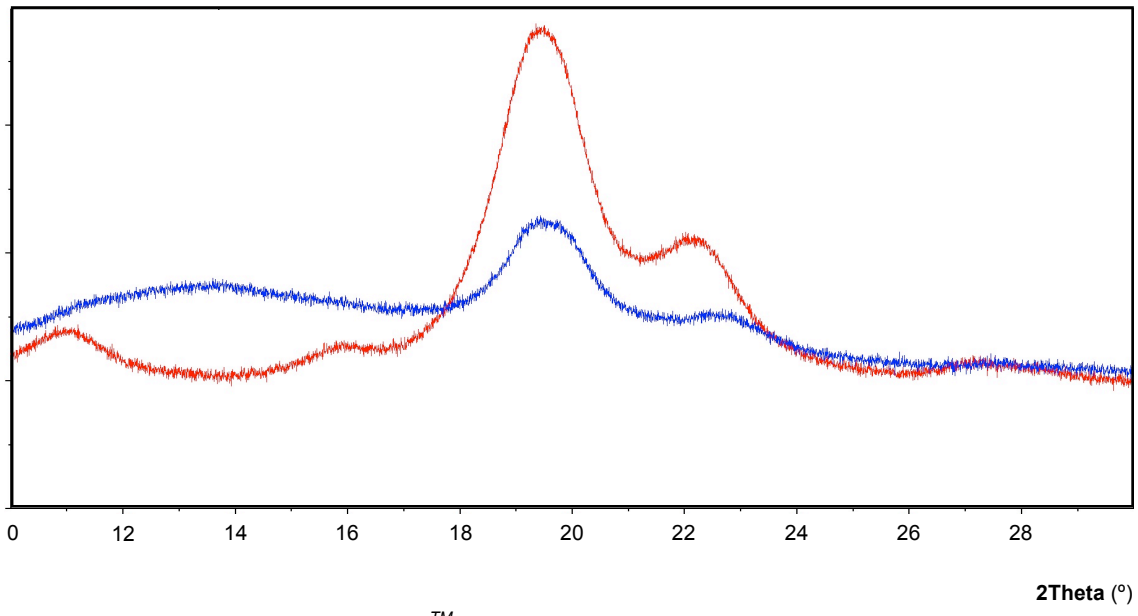

Figure 15 - Diffraction patterns of Kuralon™ PVA fibers (red line) and 99% hydrolyzed PVA powder (blue line) with the semi-crystalline peak $2\theta \approx 19°$.

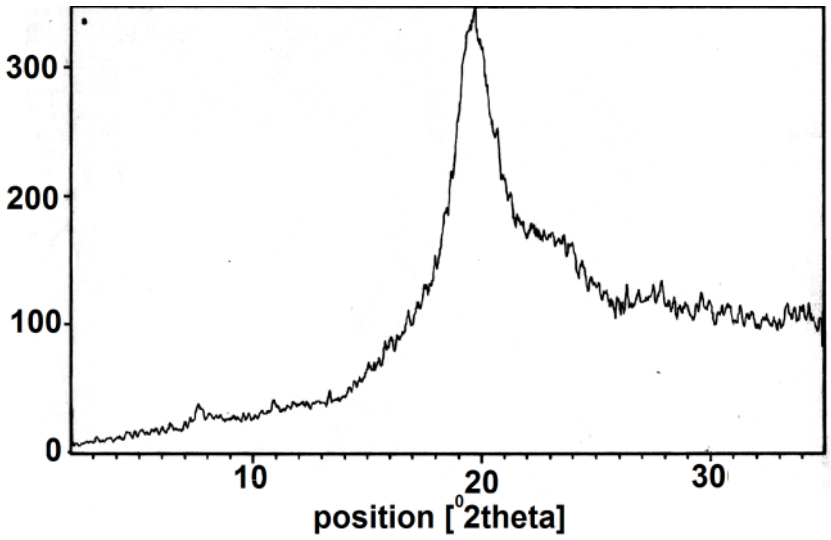

Figure 16 - Typical XRD diffraction pattern of pure PVA, as presented by Shakshooki et al. [40].

3.1.3 Inductively Coupled Plasma Optical Emission Spectrometry (ICP-OES)

In order to evaluate the *Kuralon™* fibers chemical composition a scan of 41 elements was carried out. The elements with concentration higher than 0,01ppm were took into consideration, being the ones with lower concentrations considered residual. *Kuralon™* fibers test results of ICP-OES are

presented in *Table 8.*

Table 8 - ICP-OES results for Kuralon™ fibers for elements measured expressed in ppb.

Element ($^{\text{Atomic number}}X_{\text{Atomic mass}}$)	**ppb (µg/L)**
Silicon ($^{14}Si_{29}$)	11010
Sodium ($^{11}Na_{23}$)	2213,0
Phosphorus ($^{15}P_{31}$)	2092,5
Zinc ($^{30}Zn_{66}$)	1783,5
Calcium ($^{20}Ca_{44}$)	933,45
Aluminum ($^{13}Al_{27}$)	302,70
Magnesium ($^{12}Mg_{24}$)	227,95
Potassium ($^{19}K_{39}$)	107,44
Lead ($^{82}Pb_{208}$)	104,70
Iron ($^{26}Fe_{56}$)	102,55
Mercury ($^{80}Hg_{202}$)	42,430
Barium ($^{56}Ba_{138}$)	35,890
Tungsten ($^{74}W_{186}$)	31,174
Copper ($^{29}Cu_{63}$)	21,835
Scandium ($^{21}Sc_{45}$)	18,398
Titanium ($^{22}Ti_{47}$)	12,285

Silica, sodium and phosphorus were the elements with higher concentrations. Elements such as calcium, aluminum, magnesium and potassium were present in high concentrations. Several metals as zinc, lead and mercury were reported in the analysis.

3.1.4 Scanning Electron Microscopy (SEM)

A scanning electron microscope was used to observe the morphology of *Kuraray* PVA in terms of roughness and to investigate the possibility of a coating layer on its surface.

The effect of the sterilization process in the fibers morphology was analyzed with SEM images due a possible effect caused in the fibers surface affecting the cytotoxicity assay performed following. *Figure 17* show the fiber after the sterilization under UV radiation / plasma treatment.

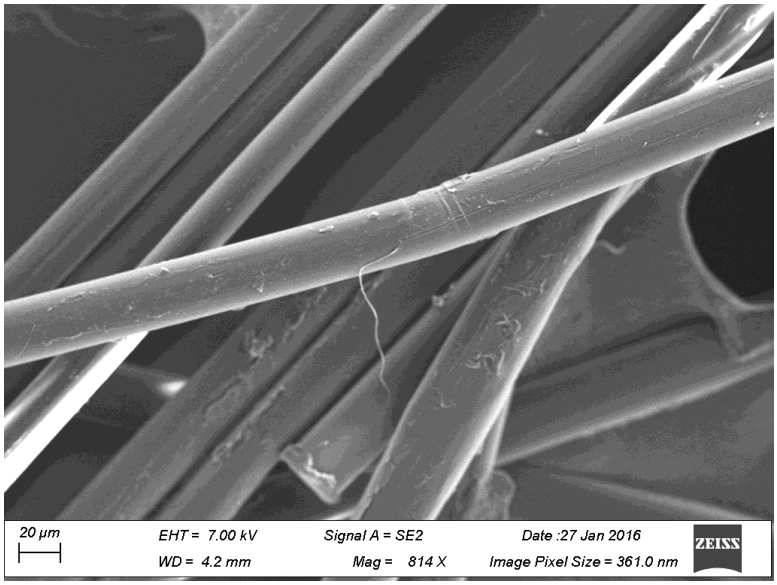

Figure 17 - Sterilized Kuralon™ fiber.

3.2 Fiber Reinforced Calcium Phosphate Cements (FRCPCs)

3.2.1 Three point bending tests

As referred in chapter 2 (materials and methods section), ten samples of each formulation were subjected to a three-point bending test, however only eight samples were selected. Due to difficulties of getting homogeneous shaped samples and after obtainment of load-displacement curves, the samples with structural visible defects and offset curves were considered outliers. The test was stopped when the load resistance of the sample or the extension of the crack reached insignificant values related with the load applied by the loading force bar in the samples. The values for each formulation are described in Table 9.

Table 9 - Values defined to stop 3 point bending test.

	Sample load resistance (N)	**Crack extension (mm)**
Control	0	0,1
1,25% 3mm	0	3,5
1,25% 6mm	2	3,5
2,5% 3mm	2	3,5
2,5% 6mm	2	3,5
5% 3mm	3	6
5% 6mm	3	6

Load-displacement (*Figure 18 - A/B/C/D/E/F/G*) curves acquired for each specimen allowed to understand the ductile and resistance properties of the different formulations. The results are presented in the chart below showing a representative behavior of each formulation.

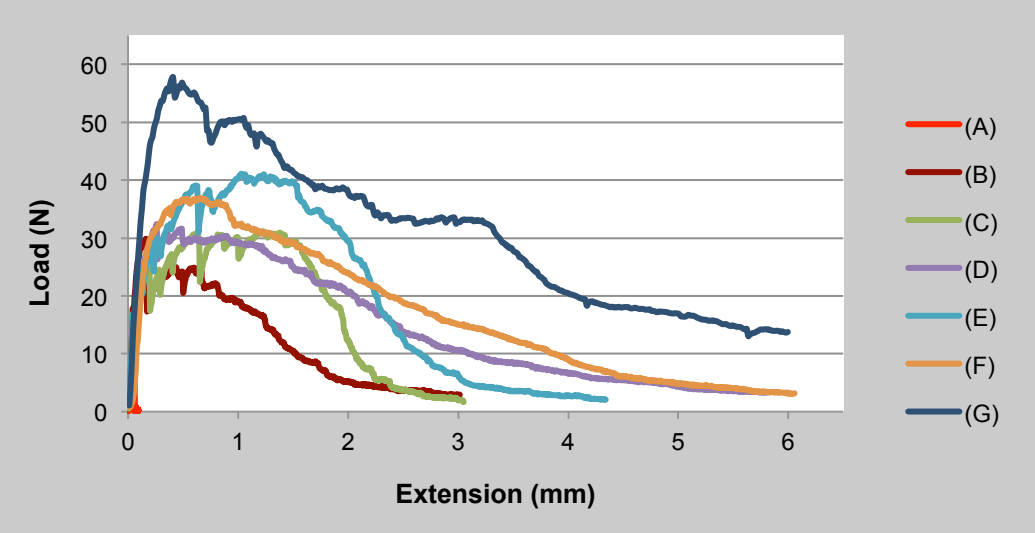

Figure 18 - Load-displacement curves representative of each formulation obtained from 3 point bending test. (A) control formulations; (B) 1.25 wt.% 3mm. (C) 1.25 wt.% 6mm formulations; (D) 2.5 wt.% 3mm formulations; (E) 2.5% 6mm formulations; (F) 5 wt.% 3mm formulations; (G) 5 wt.% 6mm formulations.

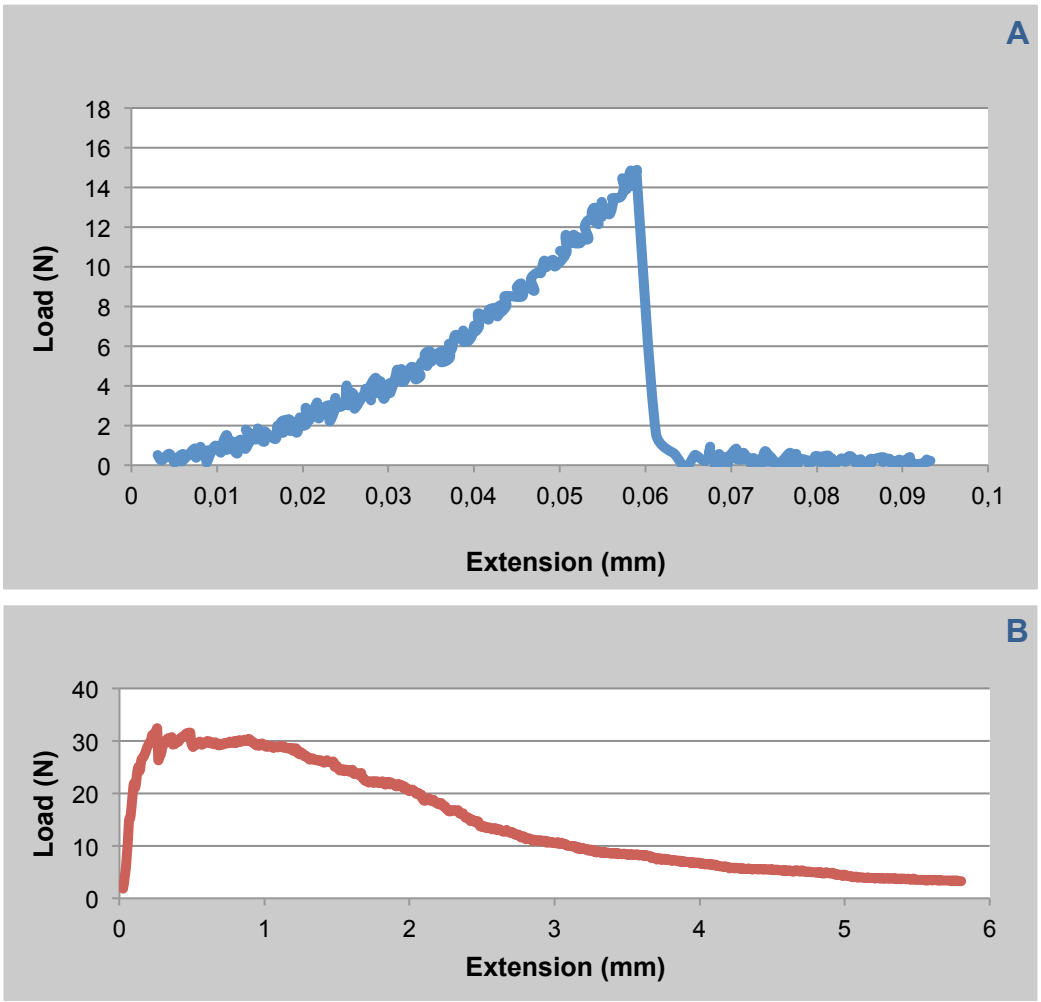

Figures 19 - (A) L-D curve of CPC. (B) L-D curve of FRCPC.

Figure 19 (A) refers to the control sample and presents the typical shape of a brittle material, with negligible deformation before the failure. On the other hand the CPCs reinforced with *Kuralon*^{TM} fibers show a behavior characteristic of a more ductile material after reached the yield point (*Figure 19 (B)*). The elastic deformation observed is obviously provided by the fibers, which helps maintaining the structure of the CPC matrix when subjected to continuous load. The amount of fibers and fiber length directly affects the maximum load supported by specimen till the yield point it's reached and thus its resistivity to support the load.

I) Flexural modulus

Figure 20 shows the flexural modulus of the specimens. At a 95% confidence interval there is not a significant interaction between the length and fiber content (p = 0,283). Therefore the significant effect of the length and fiber content was analyzed separately. For the fiber content and fiber length there are no significant differences. The p-value was 0,091 and 0,065 for the fiber content and length, respectively.

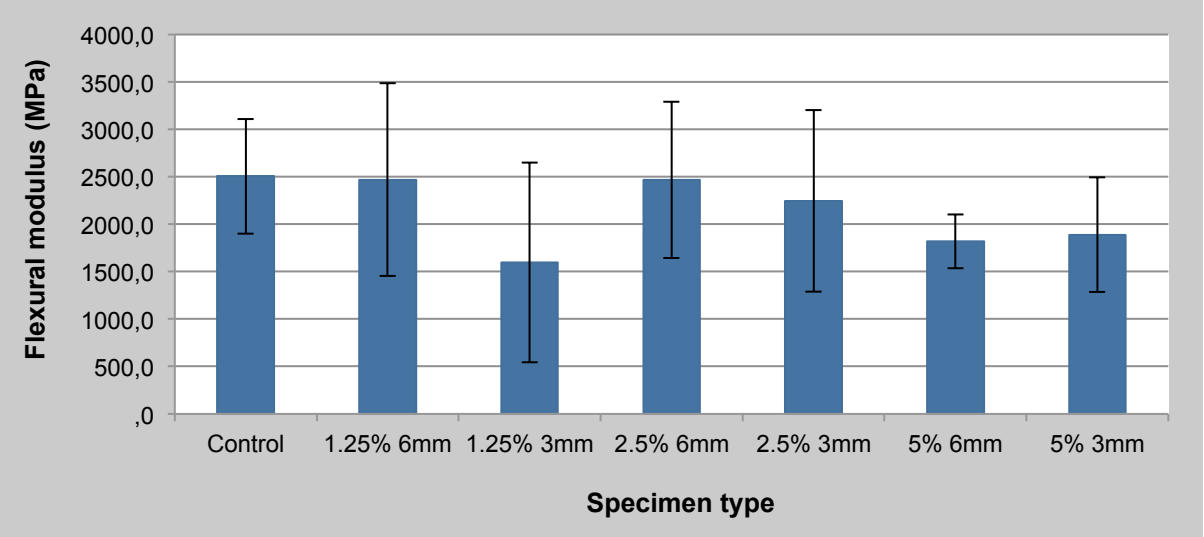

Figure 20 - Results of the flexural modulus analyzed by 3 point bending test for the control, 1.25% 6mm, 1.25% 3mm, 2.5% 6mm, 2.5% 3mm, 5% 6mm and 5% 3mm formulations.

The values observed to the flexural modulus are similar, with the 1.25% 3mm formulation presenting the lowest value (1597,4 ± 1053,25 MPa) and the control the highest (2506,2 ± 605,3 MPa). Since this mechanical property reflects the plastic behaviour of the samples, the influence of the fibers has no evident effect. No significant differences were observed in the flexural modulus of all the samples, regarding the fiber content and the fiber length. The p-value regarding the two variables is close from the acceptable stated error (5%), which means that some changes in the experimental procedure or increase the size of the sample population can be hypotheses to include this data in the confidence level.

II) Flexural strength

Figure 21 shows the flexural strength of the specimens. At a 95% confidence interval, there is not a significant interaction between the length and fiber content (p = 0,113). The significant effect of the length and fiber content was analyzed separately. For the fiber content and fiber length significant differences were observed for the flexural strength (p < 0.001).

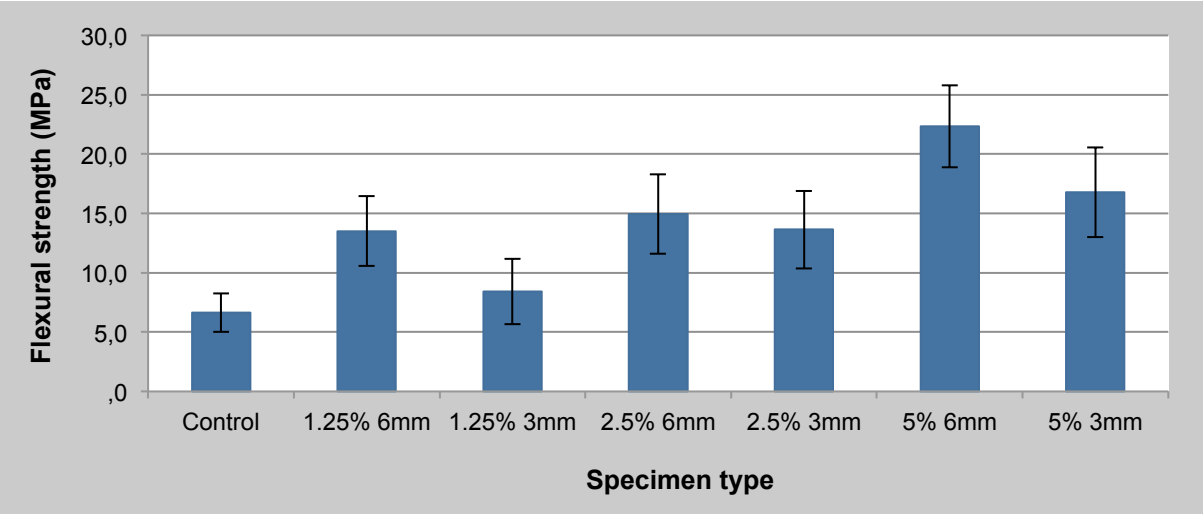

Figure 21 - Flexural strength analyzed by 3 point bending test for the control, 1.25% 6mm, 1.25% 3mm, 2.5% 6mm, 2.5% 3mm, 5% 6mm and 5% 3mm formulations.

Regarding the fiber content, the flexural strength presented significant differences between all the formulations (p < 0.05). The flexural strength increased gradually from the control till the 5 wt.% content. The control formulation presented the lowest flexural strength (6,6 ± 1,6 MPa) and the 5 wt.% (3mm; 6mm) the highest (16,8 ± 3,8 MPa; 22,3 ± 3,5 MPa). In terms of the fiber length, significant differences in flexural strength were also presented for all formulations (p < 0.001). The formulations with the same fiber content but with 6mm fibers presented high values in terms of flexural strength than the 3mm length. The analyses between the formulations with different fiber length, the control presented the lowest value (6,6 ± 1,6 MPa) and the 6mm fibers in the 5 wt.% formulation the highest (22,3 ± 3,5 MPa).

III) Work of fracture

Figure 22 demonstrates the work of fracture of the (area below the load-displacement curve) specimens when subjected to load. At a 95% confidence interval there is a significant interaction between the length and fiber content (p < 0,001).

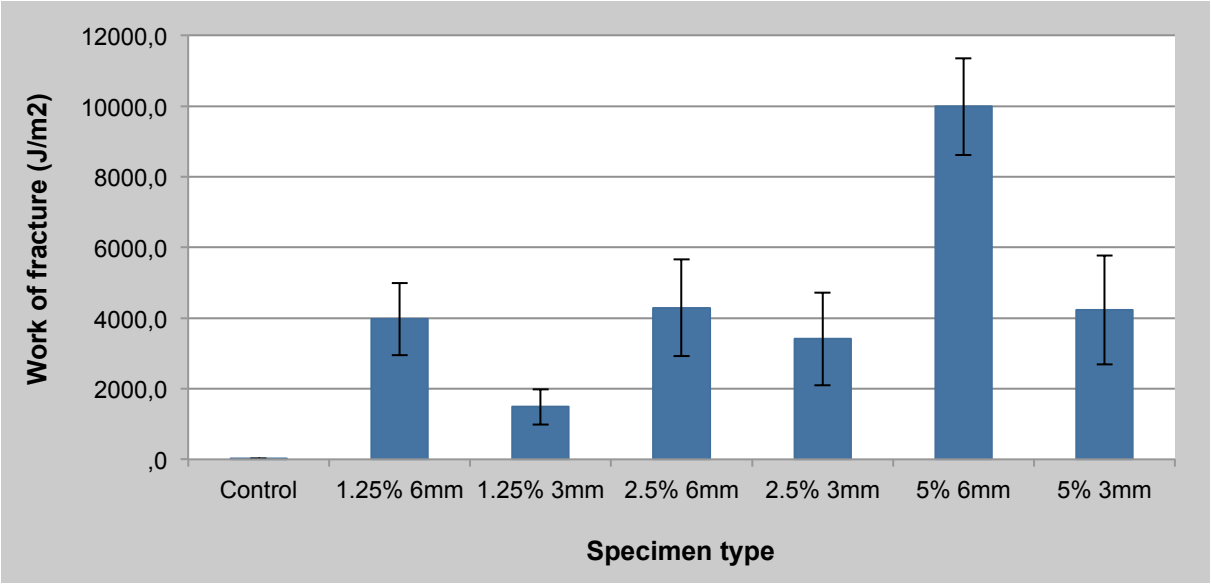

Figure 22 - Results of the work of fracture analyzed by 3 point bending test for the control, 1.25% 6mm, 1.25% 3mm, 2.5% 6mm, 2.5% 3mm, 5% 6mm and 5% 3mm formulations.

As expected, the control formulation had a brittle material behavior presenting the lowest value to work of fracture (17,4 ± 7,8 J/m^2) far from 1.25% 3mm formulation, the second lowest (1484,9 ± 501,0 J/m^2). The influence of the fiber length in the specimen work fracture is shown by the comparison of 2.5% 6mm and 5% 3mm formulations (4291,6 ± 1370,9 J/m^2; 4227,4 ± 1546,4 J/m^2, respectively) or with 1.25% 6mm and 2.5% 3mm formulations (3972,7 ± 1023,5 J/m^2; 3405,6 ± 1308,6 J/m^2, respectively). The formulation 5% 6mm showed the highest performance (9984,5 ± 1373,7 J/m^2). The fiber content proved less important for the absorption capacity of the samples than the fiber length.

3.2.2 Scanning Electron Microscopy (SEM)

Figure 23, *(A)* and *(B)* presents the random fibers orientation in the CPC matrix. The slice impressions and holes (highlighted in blue) were the consequence of the frictional sliding phenomena, leading to the fibers pullout effect. The creation of new surfaces are observable, despite the most of the fibers are still aggregate to the matrix. The interfacial transition zone (ITZ) is visible in the *Figure 23 (C), (D) and (E)*, demonstrated by the thin layer between the fiber and the matrix, manifesting some chemical repulsion that in certain way facilitates the sliding of the fiber when the composite is subjected to fracture loads. The *Figure 23 (F)* shows a crack propagating up around the fiber in a transverse direction, showing the fiber influence in the fracture process, increasing the composite strength and playing its role as a cement reinforcing. The *Figure 23 (G), (H)* show a transversal section of the *Kuralon*^{TM} fiber, which was part of a reinforced CPC after a 3 point bending test. Although is possible to visualize the existence of calcium phosphate cement traces all over the fiber, the presence of a surface coating, seems to not exist.

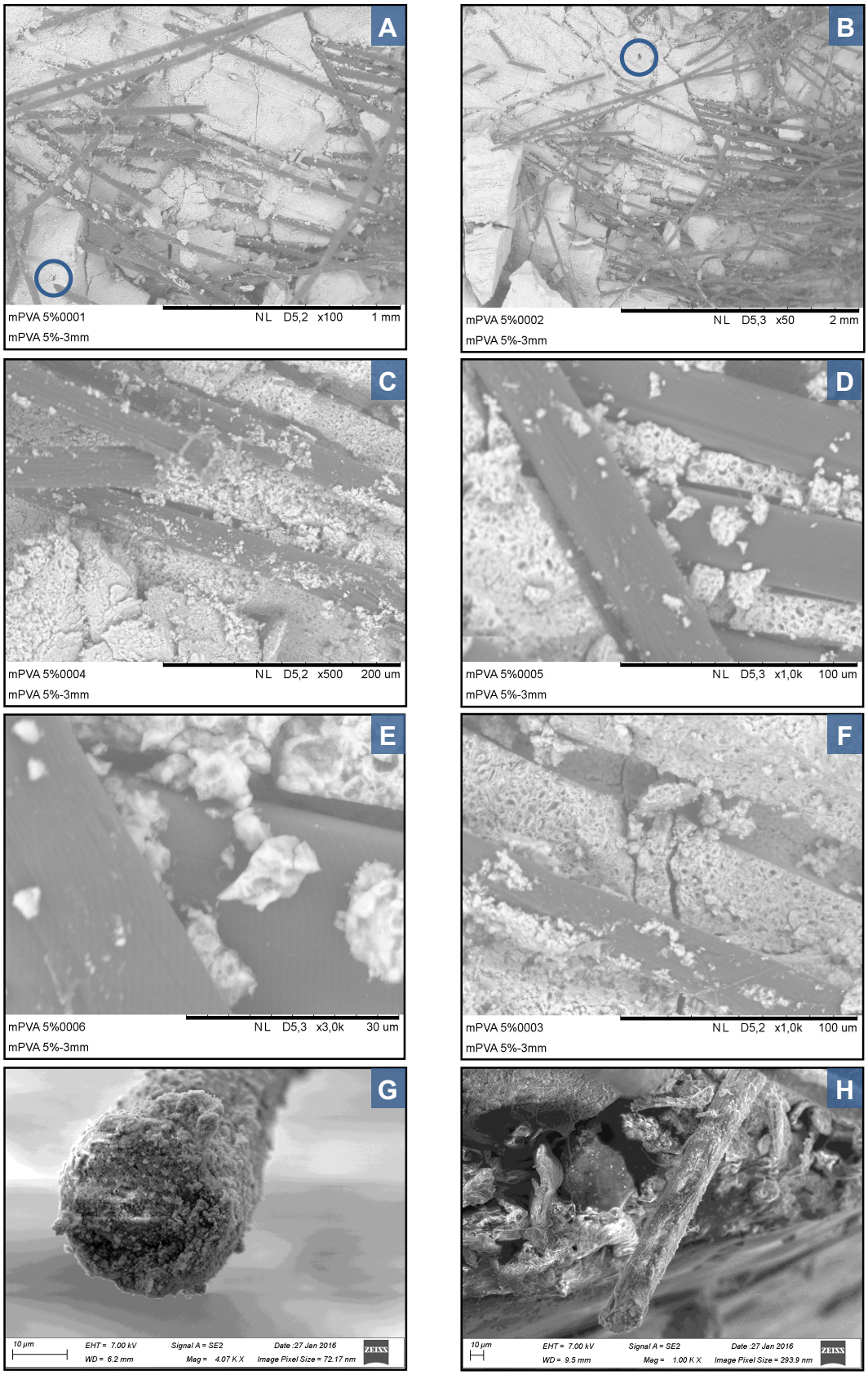

Figure 23 - SEM photos of calcium phosphate cements reinforced with Kuralon™ fibers. 5% fiber content and 3mm fiber length samples. (A), (B) - Kuralon™ fibers random dispersed in CPC matrix. Pullout and sliced fibers impress. (C), (D), (E) - ITZ layer around Kuralon™ fibers. (F) - Crack passing around the fiber. (G) - Kuralon™ fiber embedded in calcium phosphate. (H) - Non-sterilized Kuralon™ fiber incorporated in CPC matrix.

The SEM images provided a general concept of the fibers distribution in the CPC matrix as well as its action in the reinforcement of the CPC's after subjected a 3 point bending test. Overall it is clear the role of the fibers in keeping the aggregation of the matrix, enhancing its mechanical properties.

3.2.3 Micro Computed Tomography (μ-CT)

μ -CT showed the cohesion of the FRCPCs and the distribution of the fibers into the matrix in all specimens formulations. The limit of detection of μ-CT used prevented the detection of *Kuralon*^{TM} fibers, which appear as empty spaces in the CPC matrix. Only in the samples with high amount of fibers (5 wt.%) is possible its visualization. Three-dimensional μ-CT reconstruction images, helped in decoding the regions related to fibers and air bubbles (*Figure 24 (B*)). The control specimens (*Figure 24 (A))* showed relative homogenously regions with shades, probably due the setting process. In the *Figure 24 (B)* (highlighted in blue) are represented the air bubbles and shafts arising from the cements assembly. The random *Kuralon*^{TM} fibers distribution is clearly noticeable in the *Figures 24 (F)* and *(G)* through the white mists in different areas of the transversal section. The tendency to the fibers form aggregates is higher in the specimens with 5 wt.% fiber content (*Figures 24 (F)* and *(G*)) than in the 1.25 and 2.5 wt.% specimens, possibly due its electrostatic properties.

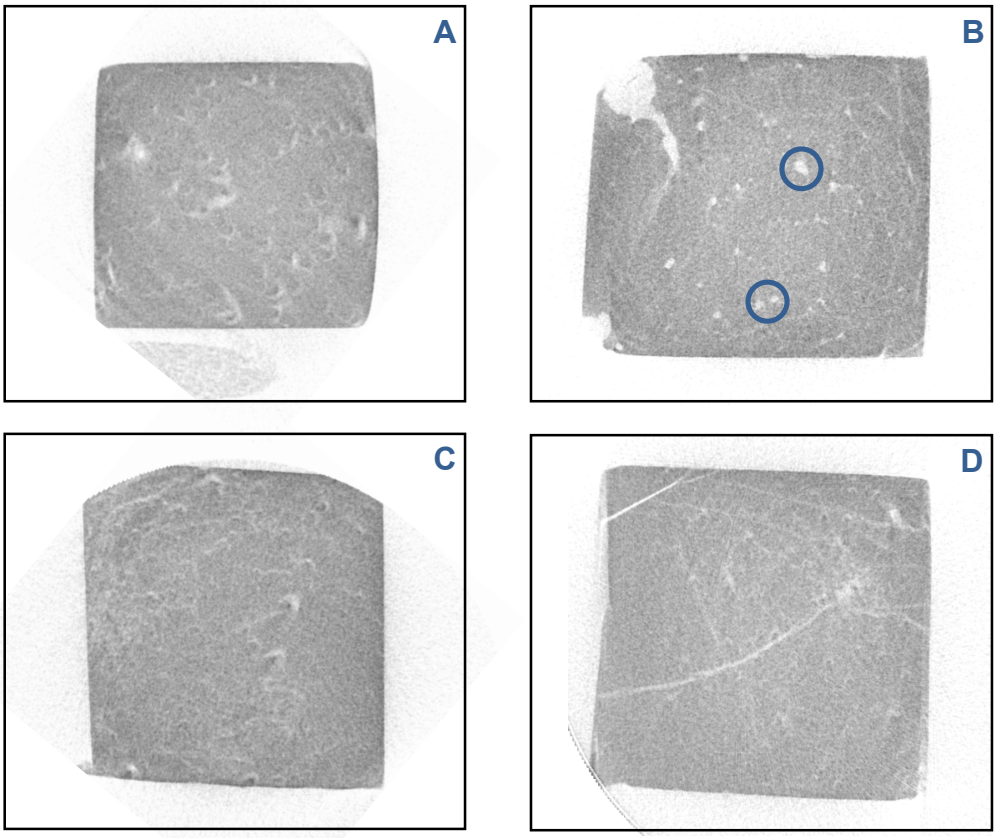

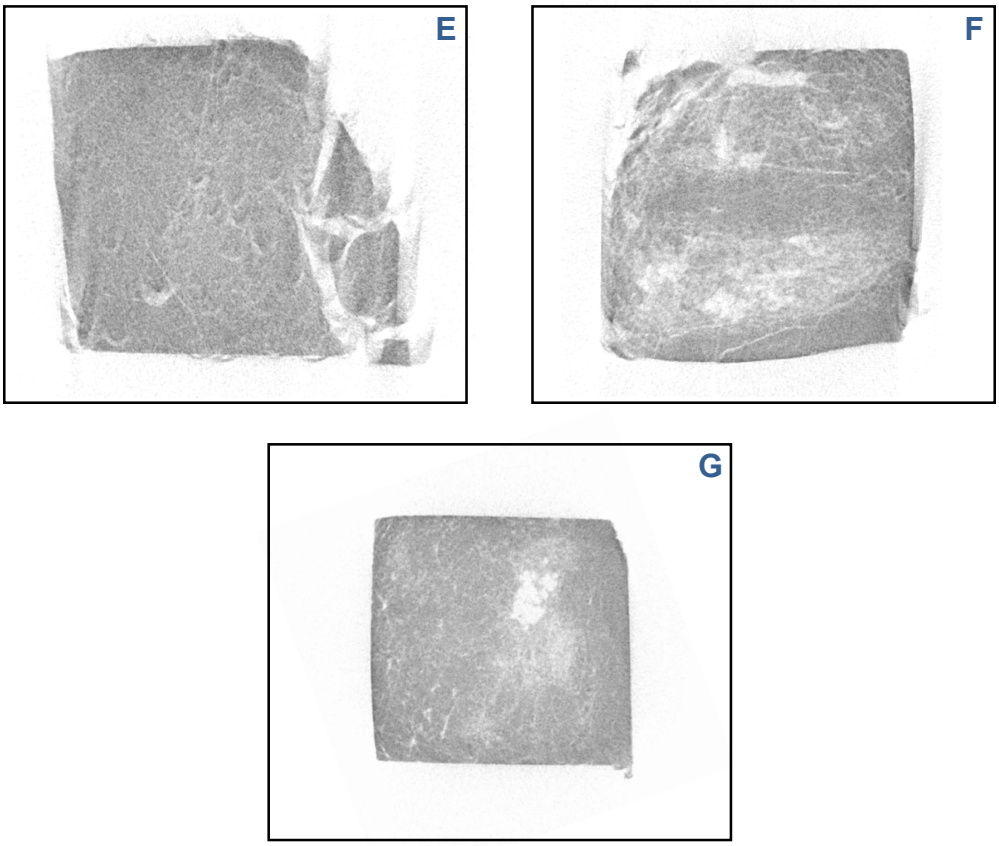

Figures 24 - μ -CT cross-section images. (A) control formulation; (B) 1.25 wt.% 3mm. (C) 1.25 wt.% 6mm formulation; (D) 2.5 wt.% 3mm formulation; (E) 2.5% 6mm formulation; (F) 5 wt.% 3mm formulation; (G) 5 wt.% 6mm formulation.

The *figures 25 (A)* and *(B)* show clearly the fibers aggregation and its distribution all over the matrix, particularly in the central longitudinal axis, as well as the formation of the air pockets.

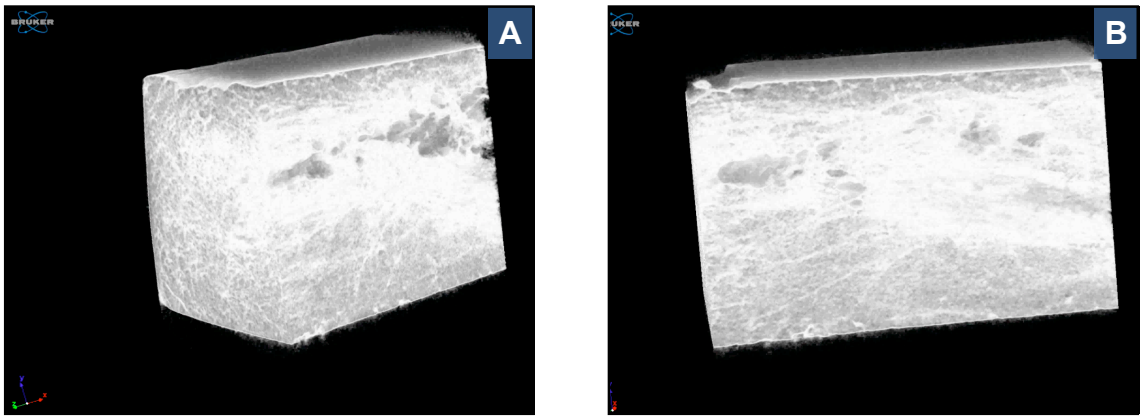

Figures 25 (A/B) - Three-dimensional μ -CT reconstruction images of 5 wt.% 6mm specimen with the air pocket and fibers hank highlighted in green and blue, respectively. (A) Transversal and longitudinal section. (B) Longitudinal section.

3.3 *Kuralon*™ cytotoxicity assay: direct and indirect contact

The figures below show the DNA concentration after different time points (24h, 48h, 72h and 7 days) for two methods of contact between the fibers and the cells, being important highlight the fact that for 7 days, the medium had been renovated twice, every 3 days.

Direct method

In the direct method, for the different fiber concentrations was observed a gradual cell growth (demonstrated by the increasing of the DNA concentration) with time. Regarding the groups with different fiber concentrations, no statistically significant differences were found in DNA concentration for the first 24h (p = 0.320), while for the 48h, 72h and 7days time points, statistically significant differences were found ($p < 0.001$).

The values of the DNA concentration for each time point and for the groups with different fiber concentration are presented in the *Figure 26*. At 24h, the DNA concentration observed for all groups with different fiber concentration (control, 0,1mg/mL, 1mg/mL and 3mg/mL) was low and similar among them, with the 0.1mg/mL group with the lowest concentration (133,1 ± 48,9 ng). At 48h was observed no significant differences in DNA concentration, except to the 1mg/mL and 3mg/mL groups (p=0,095). At 72h no significant differences were observed between the control and 0,1 mg/mL groups (p = 0,065), whereas for the other groups the difference of DNA concentration was significant (p < 0,001). After 7 days, the control group had the highest DNA concentration (2269,7 ± 43,5 ng) and the 0,1mg/mL (2230,5 ± 135,2 ng) with no statistically significant differences among them (p = 0,606). The DNA concentration on the seventh day was significant lower for 1mg/mL (1726,8 ± 47,4) and 3mg/mL (1028,2 ± 212,0 ng) groups. Over time, the DNA concentration gradually increased for each fiber concentration group.

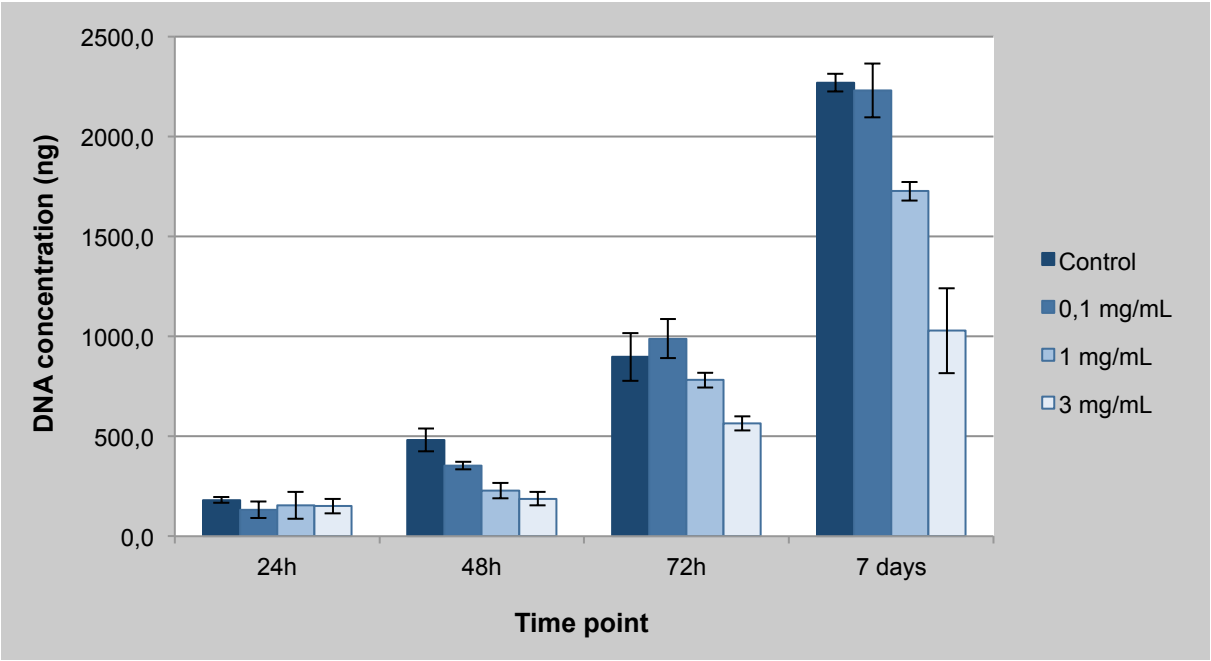

Figure 26 - DNA concentration of each fibers concentration in direct contact with M3CT3 cells at the different time points.

Indirect method

As observed in *Figure 27*, the DNA concentrations to the indirect method were very low, mainly till the third day. Over the entire period that the cells were in contact with the medium, the DNA concentration for each fiber concentration groups, did not show a gradual behavior. Regarding the groups with different fiber concentrations, statistically significant differences ($p < 0.001$) were found in the DNA concentration for the time points (24h, 48h, 72h and 7 days).

After the first 24h, no significant DNA concentration differences were observed between the groups with fibers ($p > 0.05$), and the 3mg/mL group with the lowest DNA concentration (3,7 ± 2,4 ng). At 48h time point, no significant DNA concentrations were found between the control and 1mg/mL groups (p = 0,601) and between the 0,1mg/mL and 3mg/mL groups (p = 0,251). At 72h no significant DNA concentrations were observed between control, 1mg/mL and 3mg/mL groups ($p > 0.05$). After 7 days, the DNA concentration increased and remained a tendency to no significant DNA concentrations were observed between control, 1mg/mL and 3mg/mL groups ($p > 0.05$) and 0.1mg/mL group with the highest DNA concentration (188,0 ± 71,3 ng).

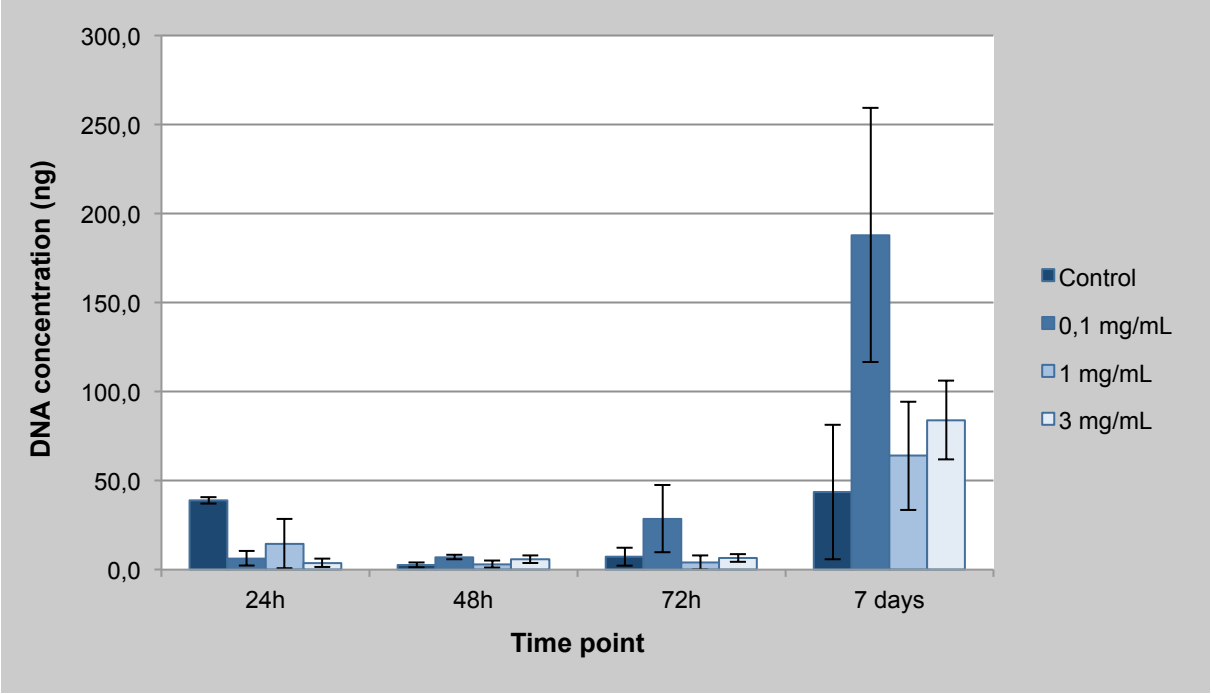

Figure 27 - DNA concentration of each fibers concentration in indirect contact with M3CT3 cells at the different time points.

Overall the DNA concentrations obtained for the direct method were substantially higher than the one for the indirect method, being in several cases approximately 10 times superior. The DNA concentration showed a gradual increase in the direct method while the indirect method several oscillations were observed over time.

chapter 4
discussion

4.1 Composition of *Kuralon*™ PVA fibers

Kuralon™ PVA fibers are described as suitable and highly efficient in concretes reinforcement for civil engineering, which raised interest in its use for the CPCs reinforcement to apply in load bearing sites. Given those good properties, the incorporation of microsized PVA fibers into calcium phosphate cements is an innovation for biomedical application. Were performed several studies to evaluate of *Kuralon*™ PVA fibers composition.

FTIR analysis was performed to investigate the molecular structure of *Kuralon*™ PVA fibers, when compared with typical PVA spectra from 99% hydrolysed PVA powder. The spectra obtained appear very similar in all the wavelength range scanned, exhibiting the same absorption bands, although minor differences are notorious in transmittance (%), probably related with the fact that the *Kuralon*™ PVA fibers were not grinded, not allowing the full coverage of the crystal detector, unlike PVA powder. The main difference in the spectra is noticeable between 2700-3000cm^{-1}. According with *Mansur et al.* in a study using PVA hydrogels crosslinked with GA, the two peaks within this wavelength range are associated with PVA crosslinked process with glutaraldehyde[39]. This two absorption bands of C-H stretching related to aldehydes, and duplet absorption peaks attributed to the alkyl chain. These bands are clearly visible in *Kuralon*™ PVA fibers spectrum. This can mean that the *Kuralon*™ PVA fibers may have been prepared with a crosslinking agent that promotes intramolecular bonds between PVA polymer chains and improving consequently the mechanical properties. However, previous studies[39] showed that the reaction of the PVA with the GA results in a considerable reduction of the intensity of the O–H (v = 3330–3350 cm^{-1}) peaks, which was not verified. The crosslinking agent used by *Kuraray* should not have been other than GA. Summarizing, *Kuralon*™ PVA fibers in comparison with 99% hydrolysed PVA powder, has a similar molecule structure, however it has undergone a crosslinking process.

X-ray diffraction test was performed in an attempt to understand the molecular arrangement differences between the *Kuralon*™ PVA fibers and the 99% hydrolysed PVA powder, as a complement to the FTIR analysis. The patterns obtained were, as expected, quite similar between them. The diffraction patterns shows a broad peak around 2θ=19,5° typical of PVA semi crystalline structure. The *Kuralon*™ PVA fibers pattern shows more intensity than 99% hydrolysed PVA powder for that angle. According with Hema *et al.*[41] the increase in broadness of the peak reveals the amorphous nature of the complex system, revealing the higher crystalline structure of *Kuralon*™ PVA fibers[41]. Probably, the crosslinking process conferred this molecular spatial organization.

The ICP-OES results showed several chemical elements that are not part of the PVA composition. The presence of this elements could be influenced by the fact that *Kuralon*™ PVA fibers were dissolved in nitric acid which probably eroded the glass flask which released ions into the

solution. Silica and sodium were reported as the elements with higher concentration. Calcium, aluminum, magnesium and potassium are also elements commonly present in glass. Zinc is a metallic transition element, highly present in the solution, maybe arising from the zinc chloride solution used to crosslink the *Kuralon*^{TM} PVA fibers[42]. Other metals such as lead and mercury are present in lower concentrations. To use this method of fibers dissolution and to counter the idea that the presence of these elements come from the glass, the nitric acid concentration used to dissolve the fibers should be adjusted, dissolving the fibers and at the same time minimize the erosion of the recipient material. The fact that the *Kuralon*^{TM} PVA fibers are not a pure polymeric system and not classified as medical grade, this elements may be associated with material impurities. The high concentrations of phosphorus, for the elements analyzed in this test, may represent the predominate element in the *Kuralon*^{TM} fibers composition, which has mineral known properties, presumably to improve the molecular structure of the fiber, described as a possibility of crosslinking agent in the *Kuralon*^{TM} patent[38]. Sulfuric acid was refereed by the company as a possibility of an inorganic crosslinking agent to the *Kuralon*^{TM} PVA fibers. In the *Kuralon*^{TM} patent are described several ways and methods to produce the fibers: dissolution, stretching and crosslinking processes included several metal based compounds which may also be in the results origin[42]. A large variety of cytotoxic elements are present, however their effect in physiological environment is directly related with the concentration.

Once the *Kuralon*^{TM} PVA fibers would be subject to a cytotoxicity assay afterwards, a sterilization process using ethanol 70% and UV radiation was performed, SEM pictures did not show any changes at the fibers surface after the sterilization processes. Were captured small filaments detaching from the homogeneous and smooth fiber surface indicating its structural composition. By analyzing the cross section no coating was observed using electron microscopy.

4.2 Processability of the produced fibre-reinforced composites

Zhou et al.[43] performed a study with engineered cementitious composites (ECC) reinforced with PVA in which is highlighted the importance of mixing sequence and the fiber distribution as key factors to improve the matrix mechanical properties. Their results proved that the adjusted mixing sequence can improved the fiber distribution. The fiber distribution is refered by this research group as the main factor to enhance the cement ductility[43]. The assembly in terms of compounds mixing sequence of the CPCs was empirically improved in order to reach a good dispersion of the fibers in the matrix. The better way to incorporate the *Kuralon*^{TM} PVA fibers in the matrix was the addition of the liquid phase to the fibers and then de calcium phosphate powder. As expected, the formulations with lower fiber content, as well as those with shorter fibers proved to be easier to assemble. These parameters have been widely studied in case of systems using different fibers and whiskers[12,24] In our study, the formulations with high amount of fibers entail problems in terms of handling to modeling samples, and consequently flaws in the samples after the paste setting. To minimize this problem, is recommended increase the number of samples to decrease the impact of samples imperfections in the following tests or improve the mixing order of the fiber-reinforced cement.

4.3 Effect of the fiber content and length in the mechanical properties of the composites

The load-displacement curves explain the fibers reinforcement effect into the calcium phosphate matrix, clarifying its reinforcing effect on the material ductility and the flexural strength, particularly the behavior after reaching the yield point. The flexural modulus obtained for all the samples was very similar and represents the tendency of a material to resist fracture by bending. On the other hand, the flexural strength and work of fracture analysis, the fiber effect was strong, as proven before by *Canal et al.*[19] with some fibers such as aramide and ceramic fibers, carbon and glass. The meshes arising from the high fiber content formulations with long fibers provide a strength enhancement in linear or biaxial direction[44]. This fact could explain the high values obtained for the 5 wt.% 3mm and 5 wt.% 6mm formulations that were subjected to a uniaxial direction stress. In this study, the formulation with best mechanical performance was the 5 wt.% 6mm presenting flexural strength ≈23 Mpa and a work of fracture ≈3 MpaJ/m^2. The mechanical values obtained for polymeric PMMA reinforced cements, considered a biomaterial appropriate for use in load bearing sites[44], are far from the values obtained with for *Kuralon*^{TM} PVA fibers. For flexural strength PMMA cements reach values ≥50 MPa[44]. In 2015, Geffers *et al.*[44] showed that polyglactin fibers incorporate in different matrices with additives, reach flexural strength values around 43 MPa and a work of fracture around 11 KJ/m^2. This research group tested also non-degradable fibers, carbon, CNC and aramid with flexural strength/work of fracture 32-60 MPa/3,5-6,5 KJ/m^2; 8,2-10,5 MPa/n.a. and 7,5-13,5 MPa/0,8-6,5 KJ/m^2, respectively[44]. The mechanical properties of the composites analyzed in this study, are bellow the cements reinforced with PMMA, polyglactin and non-degradable fibers, however several parameters such as the mixing order, modification of the fiber surface and the optimization of the fiber content and length, can be improved and reach values close to the other fibers used in cements reinforcement.

SEM analysis was very useful to understand the interaction fiber/matrix, as well the role of the *Kuralon*^{TM} PVA fibers in reinforcement of the CaP matrix. Through the SEM photos was noticeable that the cement adhered well to the fibers surface increasing the cohesion and consequently, the effect of reinforcement. However, it is also visible a small ITZ around the fibers that can weaken the reinforcement function of the fibers and have high relevance in the FRCPC micromechanical characteristics[12]. The well defined fiber sliding impressions, prove some lack of affinity in the interactions fiber/matrix. Probably a surface coating could minimize this problem, enhancing the micromechanical properties. In 2012 Kruger and Groll[12] showed with PVA fibers that the tensile strain increases from 0.5 to 1% (uncoated PVA) to 4-5% by applying 1.2% of oiling/lubricating coating on the hydroxyl groups.

The fibers have the tendency to disperse randomly in the matrix and its strength is evident when the crack is propagating in the CaP matrix and stops when reaching the fiber. This phenomenon has been well established by Zang *et al.*[9] and is responsible for the improvement of the mechanical

properties of the cement since the energy expended in the propagation of the cracks is higher, given the fact that it does not cross the fiber.

μ-CT was performed in order to get an overview of the consistency of FRCPCs. The pictures obtained from this analysis allowed realize the air bubbles presence into the samples as well the distribution of the *Kuralon*^{TM} PVA fibers into the CaP matrix. Given that, the *Kuralon*^{TM} PVA fibers have the tendency to form fiber bundles and create agglomerates, this fact is visible in the FRCPCs, particularly in the 5% wt. fibers content formulation. Possibly the air bubbles mostly present in these formulations are correlated with this fact. *Zhou et al.*[43] emphasized the fact that the adjusted mixing sequence can improve the fiber distribution. This group research also proved that in order to separate the fiber bundles and to mix fibers uniformly, high plastic viscosity of cement before fiber addition is desirable, once they used a different mixing sequence (powder-liquid-fibers-powder+liquid)[43]. The adjustment to future works it is a possibility in order to use formulations with high fibers amount but getting better fibers distribution.

4.4 Cytocompatibility of the developed fibre reinforced composites

The cytotoxicity assay revealed a greater viability in the direct contact method as compared to the indirect method. In the direct method, the lowest concentration of fibers (0,1mg/mL) proved not affect cell viability with values of DNA concentration very similar with the control group. On the other hand, the 1mg/mL and 3mg/mL concentrations, affected cell viability, especially from the second day of contact on, where is denoted a lower increase when comparing with the two other groups. Regarding the indirect method, the cell viability was extensively lower than when comparing with the direct method, generally 10 times or less. After the third day, an increase in DNA concentration was registered, corresponding to the time when the medium was renewed. The impoverishment of the medium properties, regarding the nutrients to feed the cells, may have occurred during the incubation period in which the fibers were in contact with the medium for one week. At the contact moment of the cells with the medium, this one couldn't have sufficient nutrients to feed the cells, observing very low DNA concentrations. Thus, the indirect method should not be taken into account as a relevant cytotoxicity test. Previous studies performed by Baker *et al.*[33] showed that PVA based hydrogels were biocompatible and stable *in vivo,* indicating the possible success with PVA fibers.

chapter 5
conclusions and future perspectives

Kuralon^{TM} PVA fibers are produced by *Kuraray* to be useful for industrial materials, in particular for fiber reinforced concrete but not specifically for clinical use. However, given the results obtained in this preliminary study, a deeper knowledge of its characteristics was achieved allowing the *Kuralon*^{TM} PVA fibers valorization in the biomedical field more specifically in the fiber reinforcement calcium phosphate cements area, for load bearing sites.

This study show that no significant differences were noticed in chemical composition between *Kuralon*^{TM} PVA fibers and 99% hydrolysed PVA powder using FTIR and XRD analyses. *Kuralon*^{TM} PVA fibers improved significantly the mechanical properties of CPCs, such as the cracking resistance in tension, ductility and energy absorption capacity.

In terms of cytotoxicity, it was observed that *Kuralon*^{TM} PVA fibers were not toxic to M3CT3 cells, indicating that these systems may have potential for use in clinical application. However, it is important to note that *Kuralon*^{TM} PVA fibers are not resorbable and therefore not appropriate as resorbable bone regeneration system.

In the future, much more research is needed to understand the *Kuralon*^{TM} PVA fibers properties for possible use in clinical procedures, as reinforcement of calcium phosphate cements for load bearing areas.

In terms of chemical composition, a detailed analysis including the comparison with other PVA commercial available products could be important to realize the impact of the fibers in the implant site, with respect to the long term contact with cells and secondary effects in the surrounding tissues. It would be relevant to evaluate the long-term cytotoxicity behaviour of the fibers once its long term permanence in the physiological environment can trigger unwanted autoimmune responses.

Regarding the fiber/matrix interaction into these composites, the preparation method of FRCPCs could be improved by adjusting the mixing sequence as well the treatment of the fibers to avoid the formation of aggregates and improve the fiber distribution in the matrix, in an attempt to obtain a more consistent cement, in terms of porosity and fibers distribution. Variations related with the amount and length of the fibers should be tested to optimize the mechanical properties. In an approach to clinical application, the evaluation of the setting time of the FRCPCs and the submersion of the samples in PBS, recreating the physiological environment, and the subsequent effect in mechanical properties. Regarding the enhancement of FRCPCs mechanical properties, suitable for load bearing areas, other methods for the mechanical characterization under dynamic conditions are needed to test cyclic stress, in an approach to the real condition.

references

1. Rho, J. Y., Kuhn-Spearing, L. & Zioupos, P. Mechanical properties and the hierarchical structure of bone. *Med. Eng. Phys.* **20,** 92–102 (1998).
2. Stevens, M. M. Biomaterials for bone tissue engineering. *Mater. Today* **11,** 18–25 (2008).
3. Buckwalter, J. A.; Glimcher, M. J.; Becker, R. R. Bone biology. *J. Bone Jt. Surg. (Intructional Course Lect.* **77,** 1256–1275 (1995).
4. Canalis, E., Economides, A. N. & Gazzerro, E. Bone morphogenetic proteins, their antagonists, and the skeleton. *Endocr. Rev.* **24,** 218–235 (2003).
5. Giannoudis, P., Dinopoulos, H. & Tsiridis, E. Bone substitutes: An update. *Injury* **36(Suppl 3,** S20–S27 (2005).
6. Habibobic, P. & de Groot, K. Osteoinductive biomaterials - properties and relevance in bone repair. *J. Tissue Eng. Regen. Med.* **1,** 25–32 (2007).
7. The, F. O. R. & On, O. Bone-Graft Substitutes : Facts , Fictions , and Applications. 98–103 (2001).
8. Burg, K. J., Porter, S. & Kellam, J. F. Biomaterial developments for bone tissue engineering. *Biomaterials* **21,** 2347–2359 (2000).
9. Zhang, J., Liu, W., Schnitzler, V., Tancret, F. & Bouler, J. M. Calcium phosphate cements for bone substitution: Chemistry, handling and mechanical properties. *Acta Biomater.* **10,** 1035–1049 (2014).
10. Bohner, M., Gbureck, U. & Barralet, J. E. Technological issues for the development of more efficient calcium phosphate bone cements: A critical assessment. *Biomaterials* **26,** 6423–6429 (2005).
11. Buchanan, F., Gallagher, L., Jack, V. & Dunne, N. Short-fibre reinforcement of calcium phosphate bone cement. *Proc. Inst. Mech. Eng. H.* **221,** 203–211 (2007).
12. Krüger, R. & Groll, J. Fiber reinforced calcium phosphate cements - On the way to degradable load bearing bone substitutes? *Biomaterials* **33,** 5887–5900 (2012).
13. Vallet-Reg??, M. & Gonz??lez-Calbet, J. M. Calcium phosphates as substitution of bone tissues. *Prog. Solid State Chem.* **32,** 1–31 (2004).
14. Wagoner Johnson, A. J. & Herschler, B. A. A review of the mechanical behavior of CaP and CaP/polymer composites for applications in bone replacement and repair. *Acta Biomater.* **7,** 16–30 (2011).
15. Cao, W. & Hench, L. L. Bioactive materials. *Ceram. Int.* **22,** 493–507 (1996).
16. Ginebra, M. P., Espanol, M., Montufar, E. B., Perez, R. A. & Mestres, G. New processing approaches in calcium phosphate cements and their applications in regenerative medicine. *Acta Biomater.* **6,** 2863–2873 (2010).

17. Khashaba, R. M. *et al.* Preparation, physical-chemical characterization, and cytocompatibility of polymeric calcium phosphate cements. *Int. J. Biomater.* **2011,** (2011).
18. Lopez-Heredia, M. A. *et al.* Influence of the pore generator on the evolution of the mechanical properties and the porosity and interconnectivity of a calcium phosphate cement. *Acta Biomater.* **8,** 404–414 (2012).
19. Canal, C. & Ginebra, M. P. Fibre-reinforced calcium phosphate cements: A review. *J. Mech. Behav. Biomed. Mater.* **4,** 1658–1671 (2011).
20. Liu, W., Zhang, J., Weiss, P., Tancret, F. & Bouler, J. M. The influence of different cellulose ethers on both the handling and mechanical properties of calcium phosphate cements for bone substitution. *Acta Biomater.* **9,** 5740–5750 (2013).
21. Brandt, A. M. Fibre reinforced cement-based (FRC) composites after over 40 years of development in building and civil engineering. *Compos. Struct.* **86,** 3–9 (2008).
22. Zuo, Y., Yang, F., Wolke, J. G. C., Li, Y. & Jansen, J. A. Incorporation of biodegradable electrospun fibers into calcium phosphate cement for bone regeneration. *Acta Biomater.* **6,** 1238–1247 (2010).
23. Tosun-Feleko??lu, K., Feleko??lu, B., Ranade, R., Lee, B. Y. & Li, V. C. The role of flaw size and fiber distribution on tensile ductility of PVA-ECC. *Compos. Part B Eng.* **56,** 536–545 (2014).
24. Xu, H. H., Eichmiller, F. C. & Giuseppetti, a a. Reinforcement of a self-setting calcium phosphate cement with different fibers. *J. Biomed. Mater. Res.* **52,** 107–114 (2000).
25. Xu, H. H., Eichmiller, F. C. & Barndt, P. R. Effects of fiber length and volume fraction on the reinforcement of calcium phosphate cement. *J. Mater. Sci. Mater. Med.* **12,** 57–65 (2001).
26. Pinho, E. D., Martins, A., Ara??jo, J. V., Reis, R. L. & Neves, N. M. Degradable particulate composite reinforced with nanofibres for biomedical applications. *Acta Biomater.* **5,** 1104–1114 (2009).
27. Lee, B. Y., Kim, J. K., Kim, J. S. & Kim, Y. Y. Quantitative evaluation technique of Polyvinyl Alcohol (PVA) fiber dispersion in engineered cementitious composites. *Cem. Concr. Compos.* **31,** 408–417 (2009).
28. Torigoe, S., Horikoshi, T., Ogawa, A., Saito, T. & Hamada, T. Study on Evaluation Method for PVA Fiber Distribution in Engineered Cementitious Composite. *J. Adv. Concr. Technol.* **1,** 265–268 (2003).
29. Valadez-Gonzalez, a., Cervantes-Uc, J. M., Olayo, R. & Herrera-Franco, P. J. Effect of fiber surface treatment on the fiber–matrix bond strength of natural fiber reinforced composites. *Compos. Part B Eng.* **30,** 309–320 (1999).
30. Kingshott, P., Andersson, G., McArthur, S. L. & Griesser, H. J. Surface modification and chemical surface analysis of biomaterials. *Curr. Opin. Chem. Biol.* **15,** 667–676 (2011).
31. Xu, F. J., Neoh, K. G. & Kang, E. T. Bioactive surfaces and biomaterials via atom transfer radical polymerization. *Prog. Polym. Sci.* **34,** 719–761 (2009).
32. Zhang, C., Yuan, X., Wu, L., Han, Y. & Sheng, J. Study on morphology of electrospun poly(vinyl alcohol) mats. *Eur. Polym. J.* **41,** 423–432 (2005).

33. Baker, M. I., Walsh, S. P., Schwartz, Z. & Boyan, B. D. A review of polyvinyl alcohol and its uses in cartilage and orthopedic applications. *J. Biomed. Mater. Res. - Part B Appl. Biomater.* **100 B,** 1451–1457 (2012).
34. Krumova, M., López, D., Benavente, R., Mijangos, C. & Pereña, J. . Effect of crosslinking on the mechanical and thermal properties of poly(vinyl alcohol). *Polymer (Guildf).* **41,** 9265–9272 (2000).
35. Tadavarthy, M., Moller, J. & Amplatz, K. Polyvinyl Alcohol (Ivalon) - A new embolic material. **125,** (1975).
36. Zhang, L. *et al.* High strength graphene oxide/polyvinyl alcohol composite hydrogels. *J. Mater. Chem.* **21,** 10399 (2011).
37. Bezerra, E. M., Joaquim, A. P., Jr, H. S. & Paulo, S. Some properties of fiber-cement composites with selected fibers. *Conferência Bras. Mater. e Tecnol. Não-Convencionais – Habitações e Infra- Estrut. Interess. Soc. – Bras. NOCMAT* 33–43 (2004).
38. Masakazu, N. & Harada, Y. Polyvinyl alcohol-based synthetic fiber and process for producing the same. (1996).
39. Mansur, H. S., Sadahira, C. M., Souza, A. N. & Mansur, A. A. P. FTIR spectroscopy characterization of poly (vinyl alcohol) hydrogel with different hydrolysis degree and chemically crosslinked with glutaraldehyde. *Mater. Sci. Eng. C* **28,** 539–548 (2008).
40. Shakshooki, S. K., Elejmi, a a, Hamassi, a M. & Masoud, N. a. Facile Synthesis of Poly (vinylalcohol)/ Fibrous Cerium Phosphate Nanocomposite Membranes. *Phys. Mater. Chem.* **4,** 1–6 (2014).
41. Hema, M., Selvasekarapandian, S., Arunkumar, D., Sakunthala, A. & Nithya, H. FTIR, XRD and ac impedance spectroscopic study on PVA based polymer electrolyte doped with NH4X (X = Cl, Br, I). *J. Non. Cryst. Solids* **355,** 84–90 (2009).
42. Characteristics of KURALON TM (PVA fiber) 1 . Chemical Structure m OH Good resistance against chemicals (alkaline), Good adhesion to cement matrix. (1986).
43. Zhou, J. *et al.* Improved fiber distribution and mechanical properties of engineered cementitious composites by adjusting the mixing sequence. *Cem. Concr. Compos.* **34,** 342–348 (2012).
44. Geffers, M., Groll, J. & Gbureck, U. Reinforcement Strategies for Load-Bearing Calcium Phosphate Biocements. *Materials (Basel).* **8,** 2700–2717 (2015).